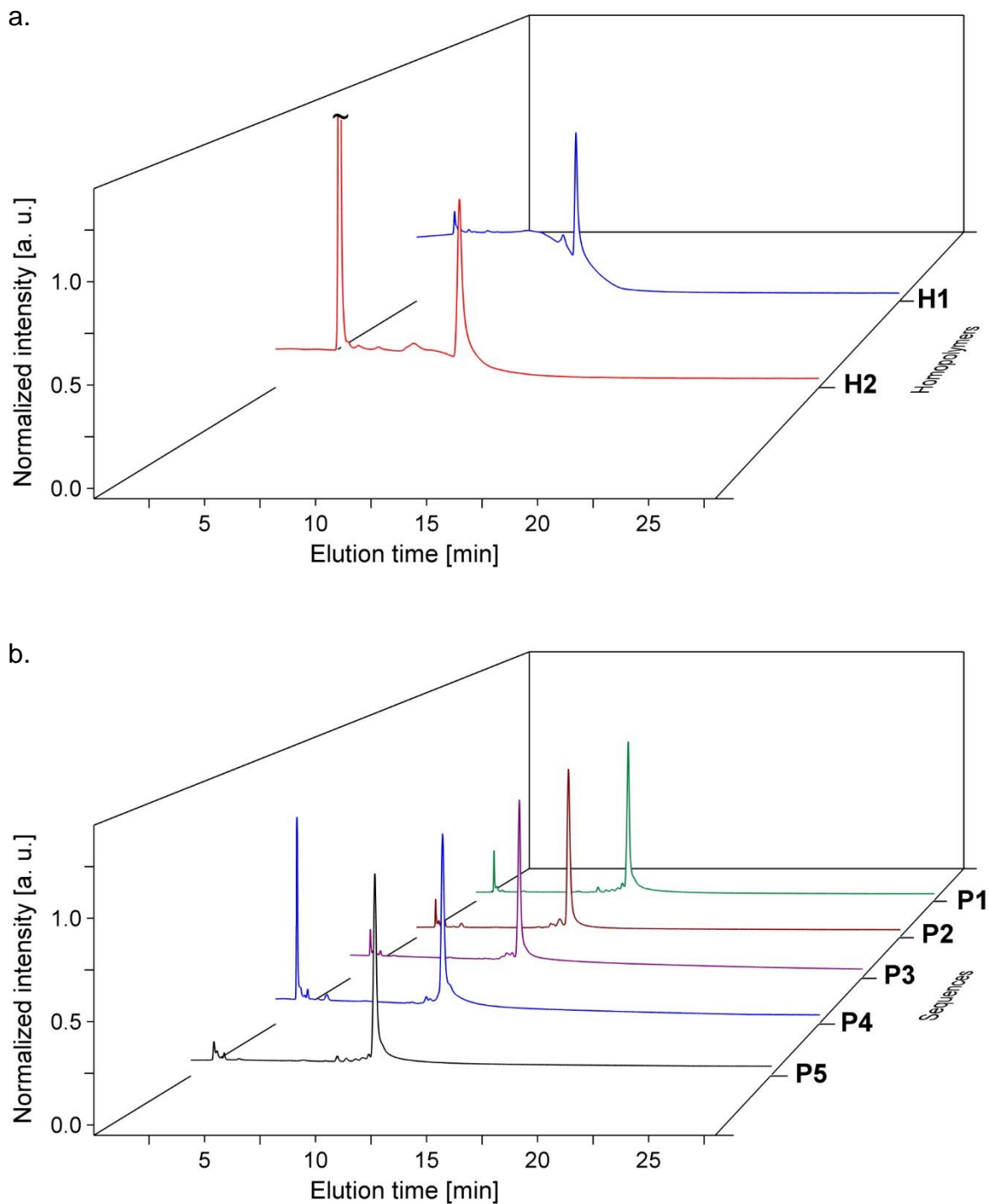
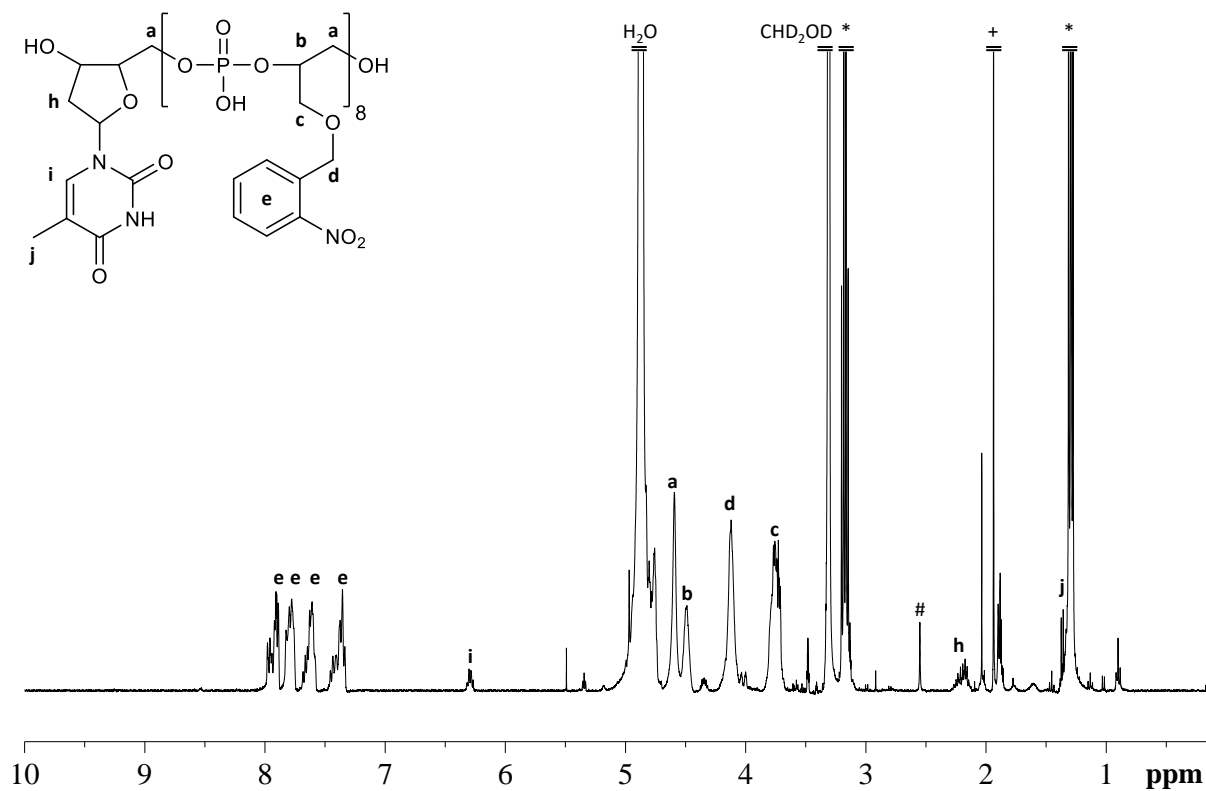


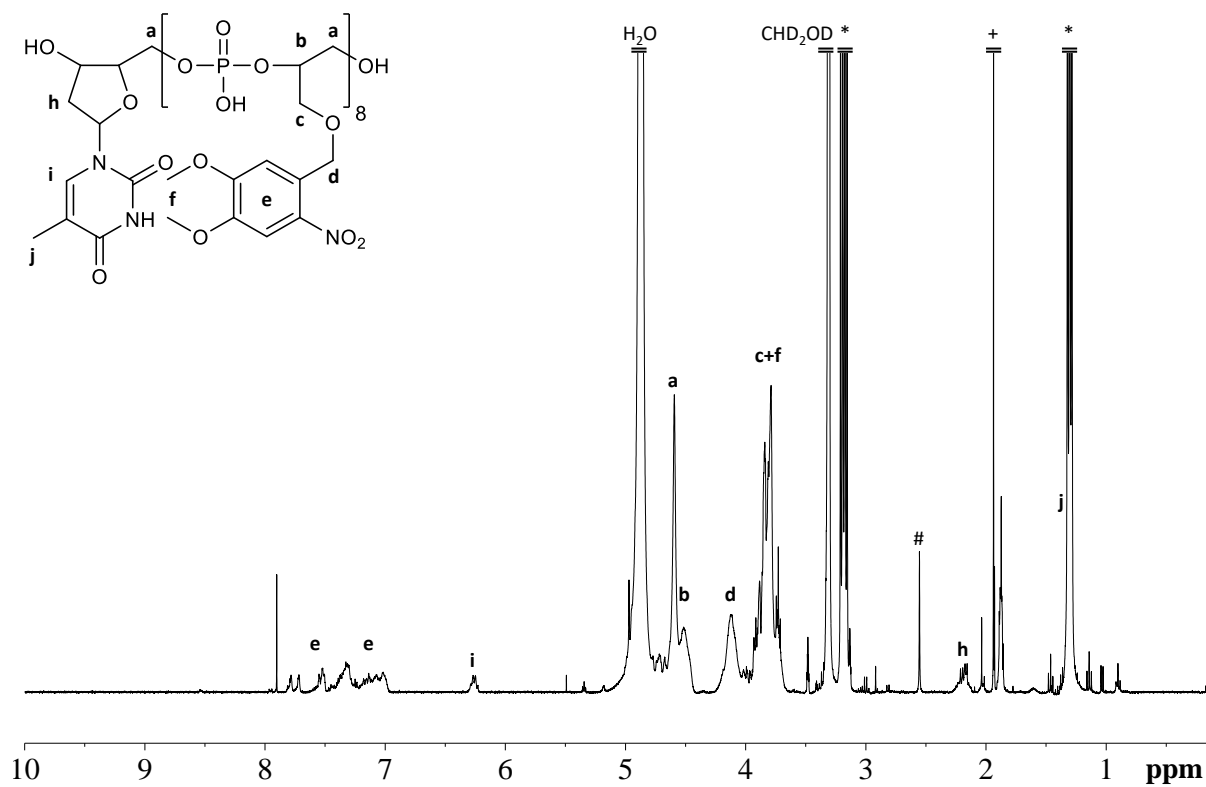
Supplementary Figures.



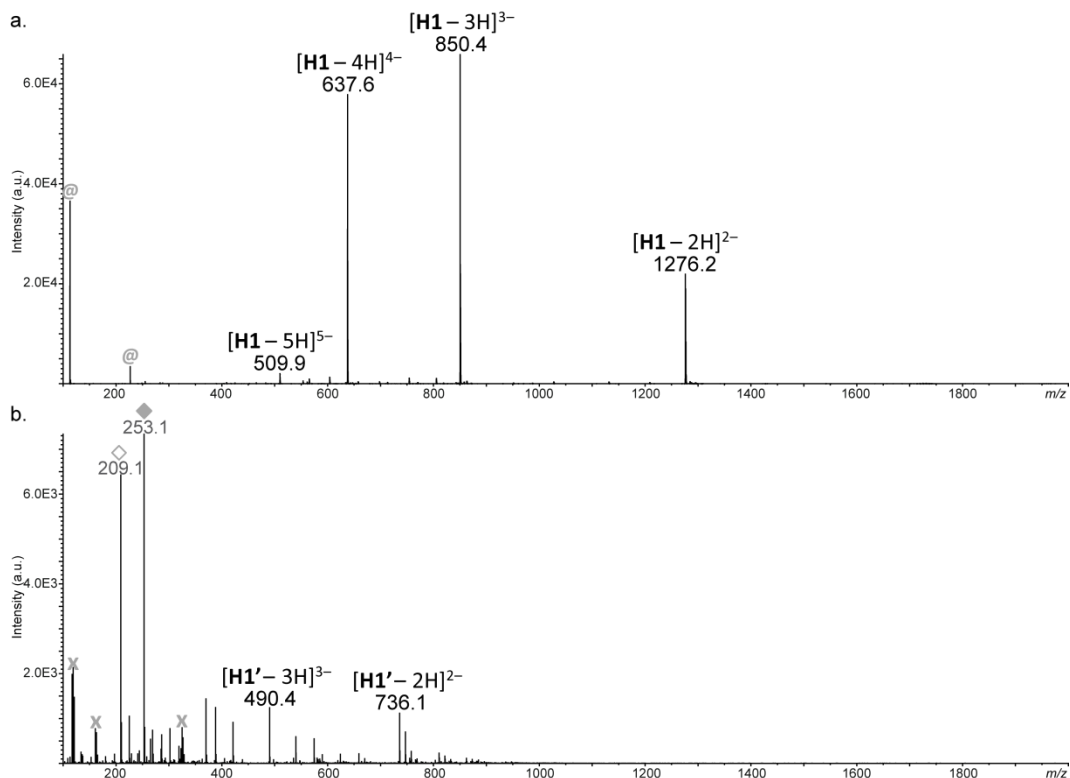
Supplementary Figure 1. IE-HPLC traces measured for (a) homopolymers **H1-H2** and (b) copolymers **P1-P5**. The chromatograms are recorded at $\lambda = 260$ nm. Experimental conditions: phase A: 10 % MeCN 20 % 2M NH_3 in water, phase B: 2.5 M NaCl in water; gradient: 0-3 min 5 % B, 3-23 min 5 % B-30 % B, 23-28 min 30 % B, 28-35 min 30% \rightarrow 5 % B; flow rate: 1 mL \cdot min $^{-1}$.



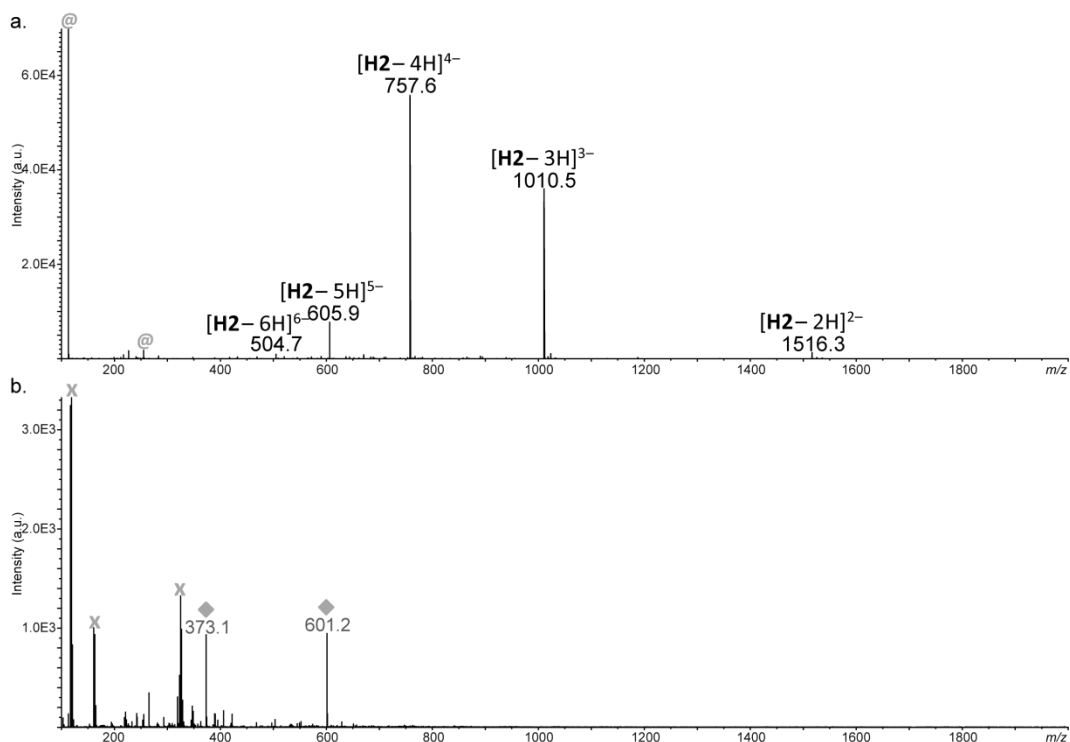
Supplementary Figure 2. ¹H NMR spectrum recorded at RT in CD₃OD for homopolymer **H1**. The star symbols indicate signals of triethylammonium counterions. (#) Methylamine, (+) acetonitrile.



Supplementary Figure 3. ¹H NMR spectrum recorded at RT in CD₃OD for homopolymer **H2**. The star symbols indicate signals of triethylammonium counterions. (#) Methylamine, (+) acetonitrile.



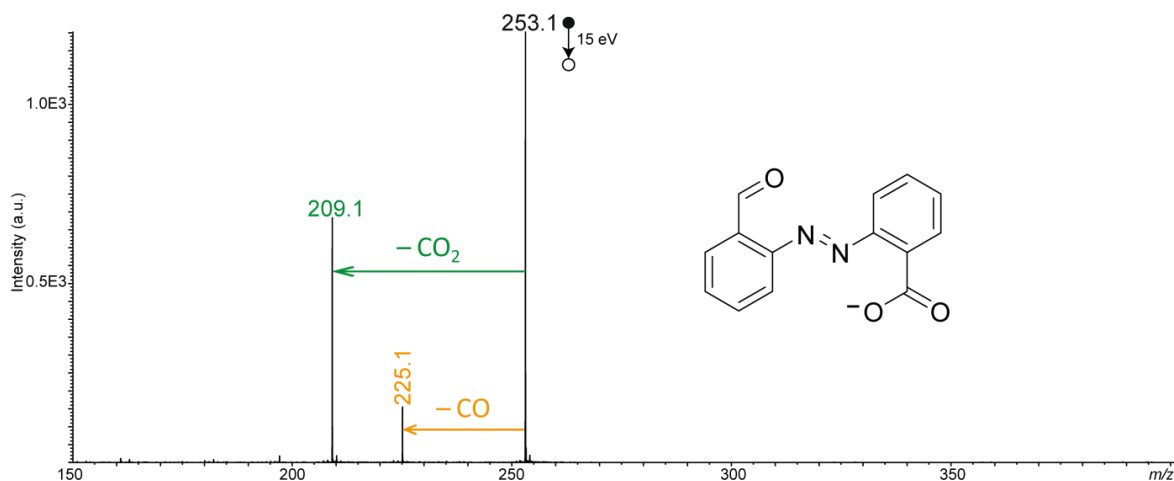
Supplementary Figure 4. ESI HRMS spectra recorded for (a) homopolymer **H1** before irradiation and (b) the resulting polymer **H1'** after photo-exposure. Grey symbols designate clusters of trifluoroacetic acid (@), of trichloroacetic acid (x) or photo-deprotection by-products (diamond).



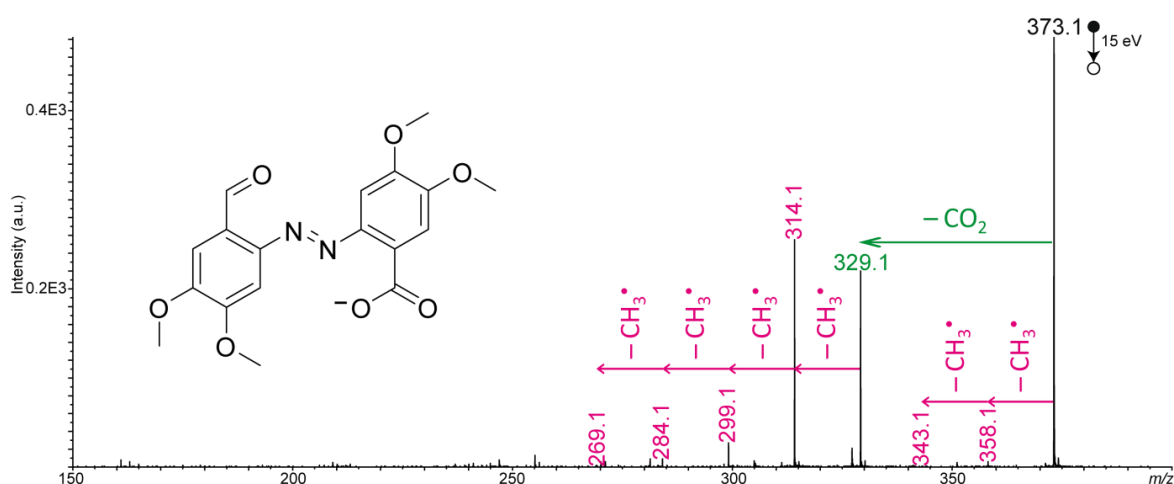
Supplementary Figure 5. ESI HRMS spectra recorded for (a) homopolymer **H2** before irradiation and (b) the resulting polymer **H2'** after photo-exposure. Grey symbols designate clusters of trifluoroacetic acid (@), of trichloroacetic acid (x) or photo-deprotection by-products (diamond).

Supplementary discussion.

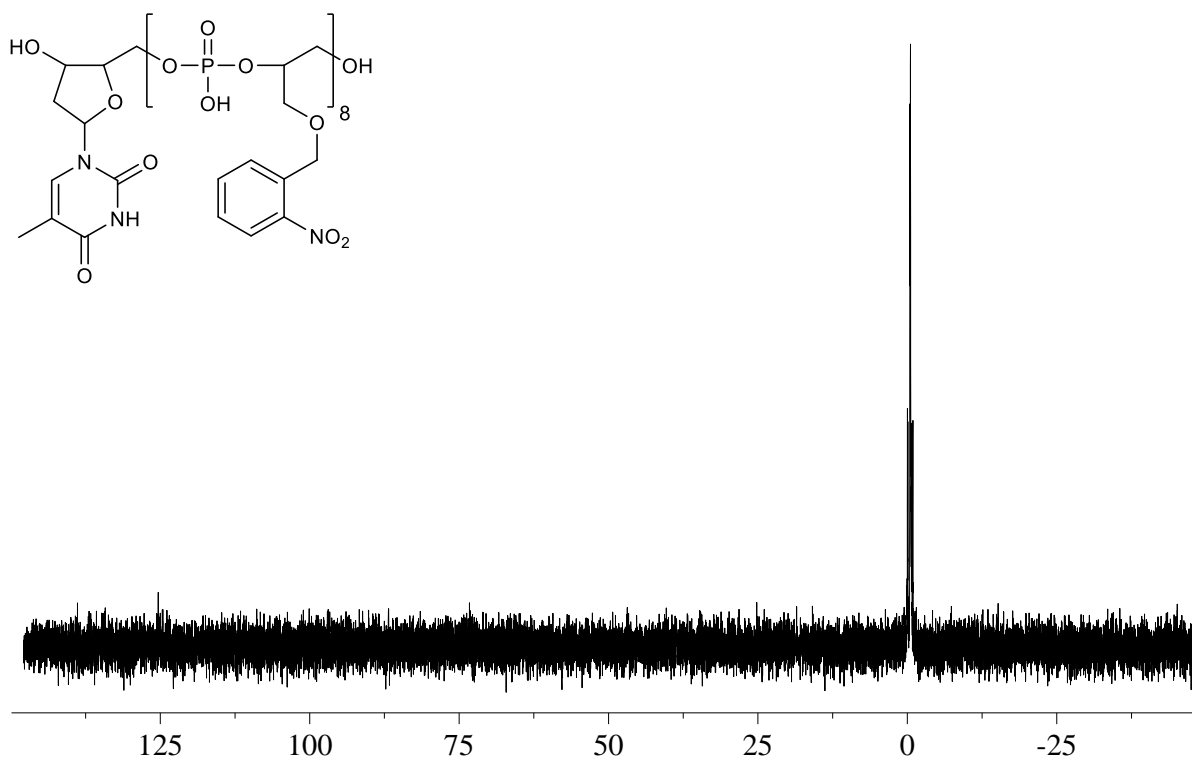
Interpretation of the photo-deprotection by-products detected by ESI HRMS. The peaks indicated by filled grey diamonds in ESI HRMS spectra of photo-exposed samples correspond to photo-deprotection by-products. As indicated in Fig. 1 of the main manuscript, nitrosobenzaldehyde intermediates are usually formed upon *o*-nitrobenzyl and *o*-nitroveratryl photocleavage.¹ However, it has been reported that these intermediates can further photo-dimerize into azobenzene diacid derivatives.^{2,3} In the present photo-deprotection and analytical conditions, the formation of dimers containing carboxylic acid and aldehyde groups was observed,⁴ as evidenced below in Supplementary Figures 6 and 7.



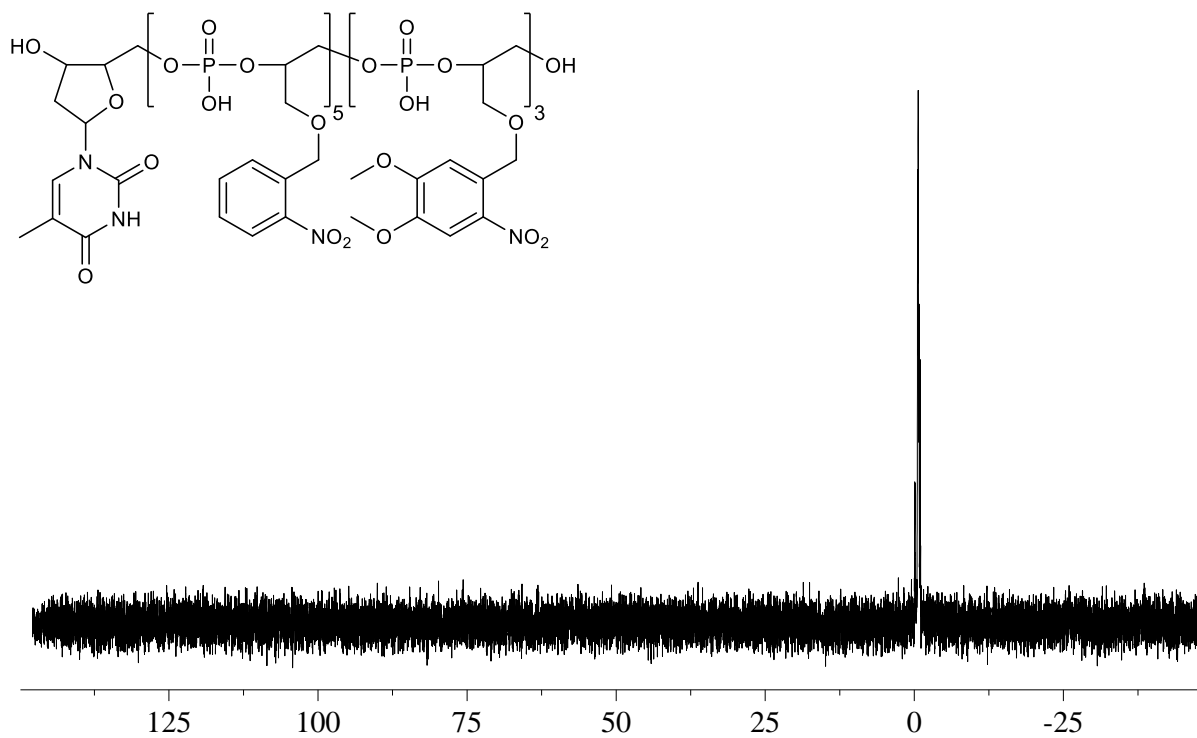
Supplementary Figure 6. MS/MS spectrum recorded for the photo-deprotection by-product observed at m/z 253.1 ($C_{14}H_9N_2O_3^-$, m/z_{th} 253.0619, m/z_{exp} 253.0614) after photo-irradiation of homopolymer **H1**, showing competitive losses of CO and CO₂ consistent with the proposed structure shown in inset. Of note, the m/z 209.1 ion labelled with an empty diamond in Supplementary Figure 4 indicates that the decarboxylation reaction also occurred during ion transfer through the interface of the mass spectrometer.



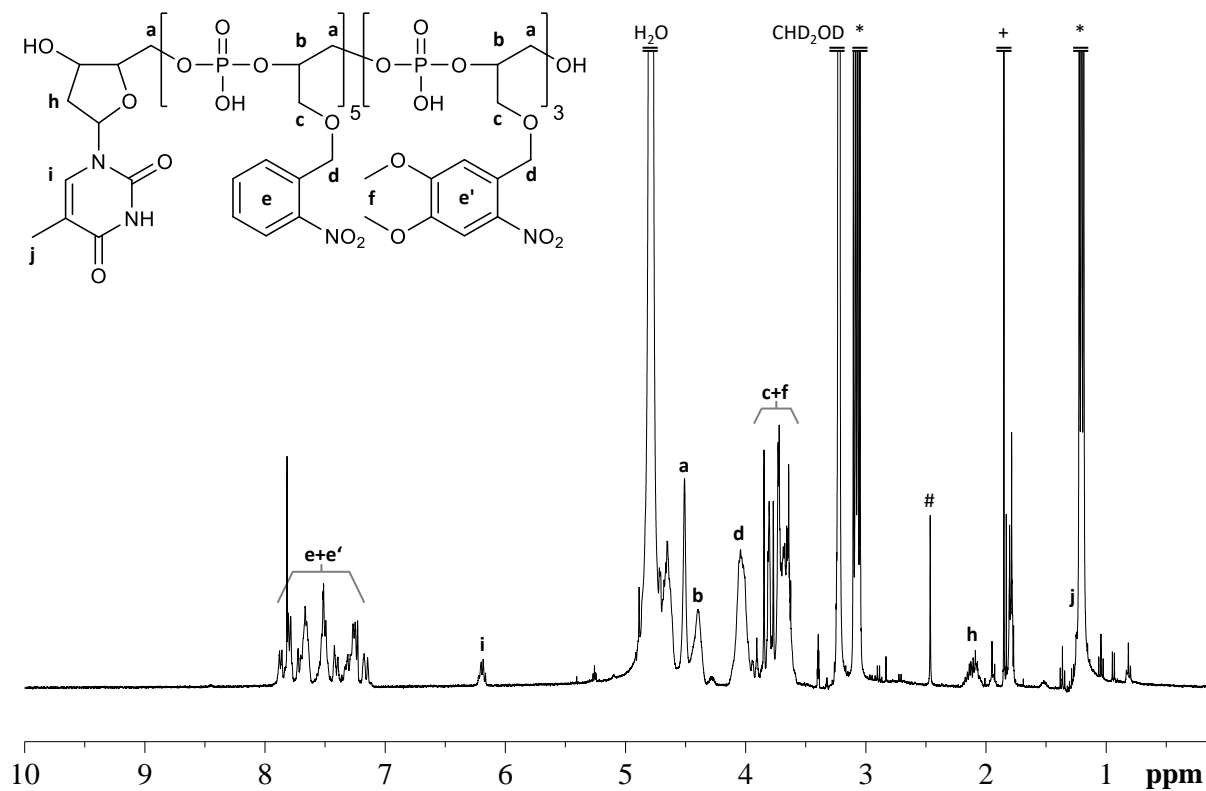
Supplementary Figure 7. MS/MS spectrum recorded for the photo-deprotection by-product observed at m/z 373.1 ($C_{18}H_{17}N_2O_7^-$, m/z_{th} 373.1041, m/z_{exp} 373.1022) after photo-irradiation of homopolymer **H2**, showing that the decarboxylation product (m/z 329.1) successively eliminates four methyl radicals, consistent with the four methoxy groups of the precursor ion (see inset structure).



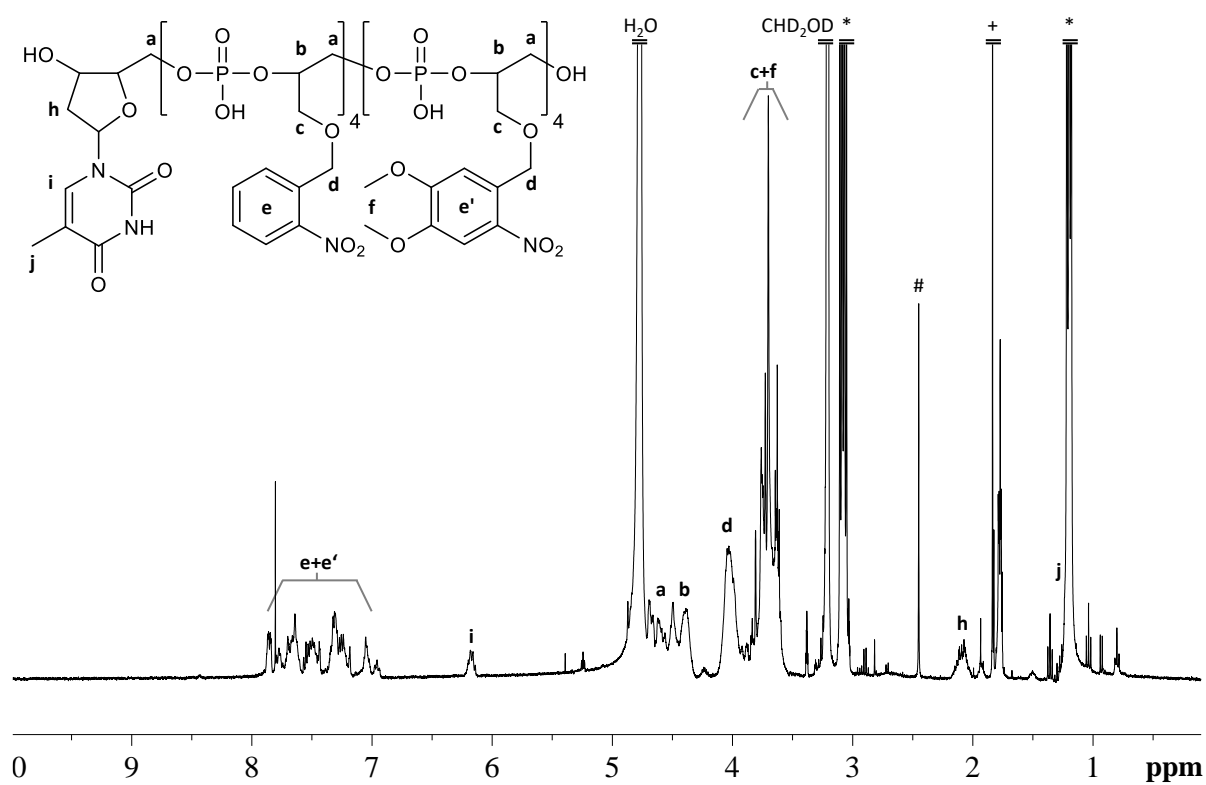
Supplementary Figure 8. ^{31}P NMR spectrum recorded at RT in CD_3OD for homopolymer **H1**. Comparable spectra were obtained for all other homopolymers studied in this work.



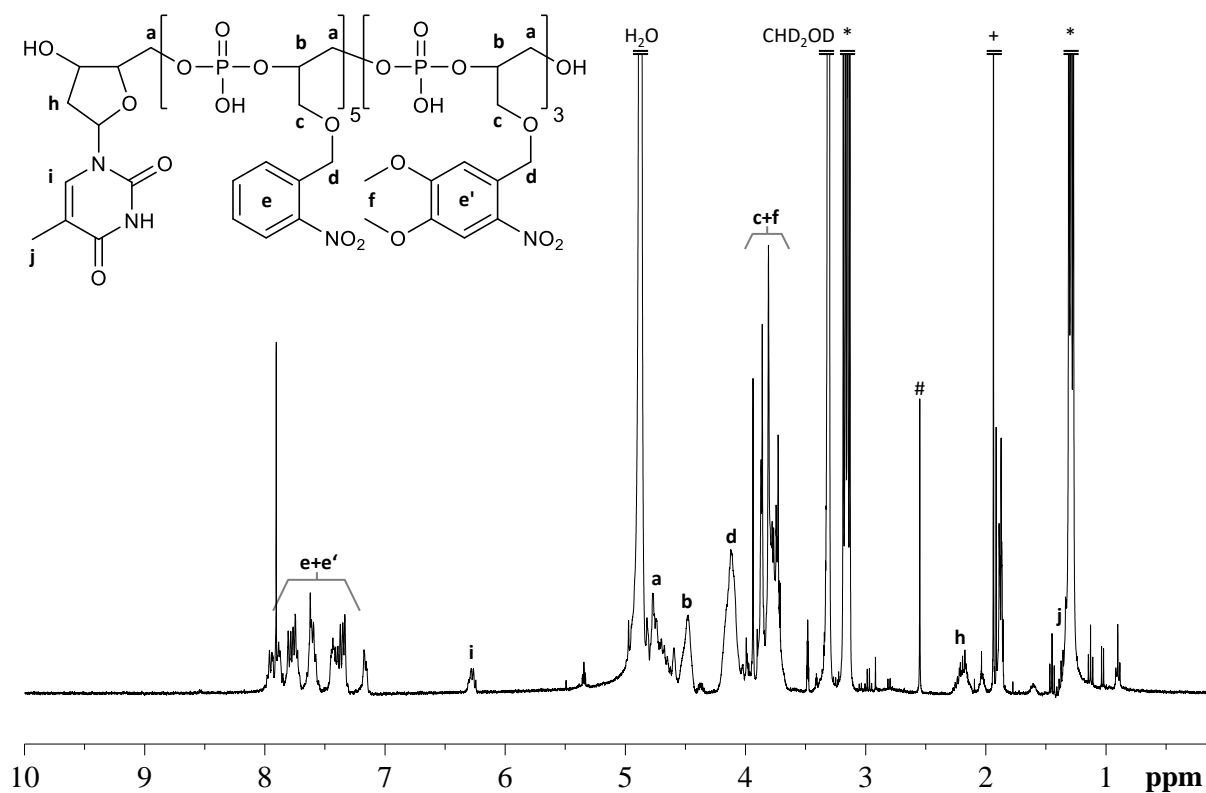
Supplementary Figure 9. ^{31}P NMR spectrum recorded at RT in CD_3OD for copolymer **P1**. Comparable spectra were obtained for all other copolymers studied in this work.



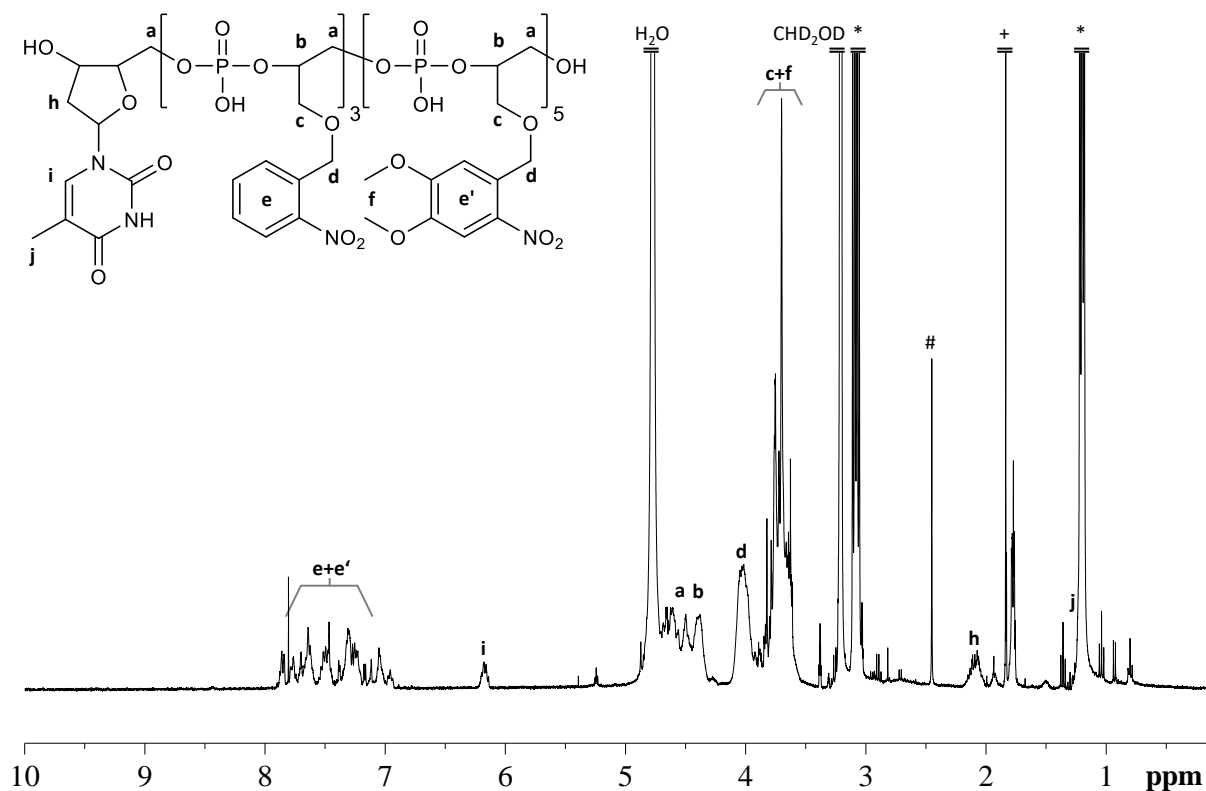
Supplementary Figure 10. ¹H NMR spectrum recorded at RT in CD₃OD for copolymer P1. The star symbols indicate signals of triethylammonium counterions. (#) Methylamine, (+) acetonitrile.



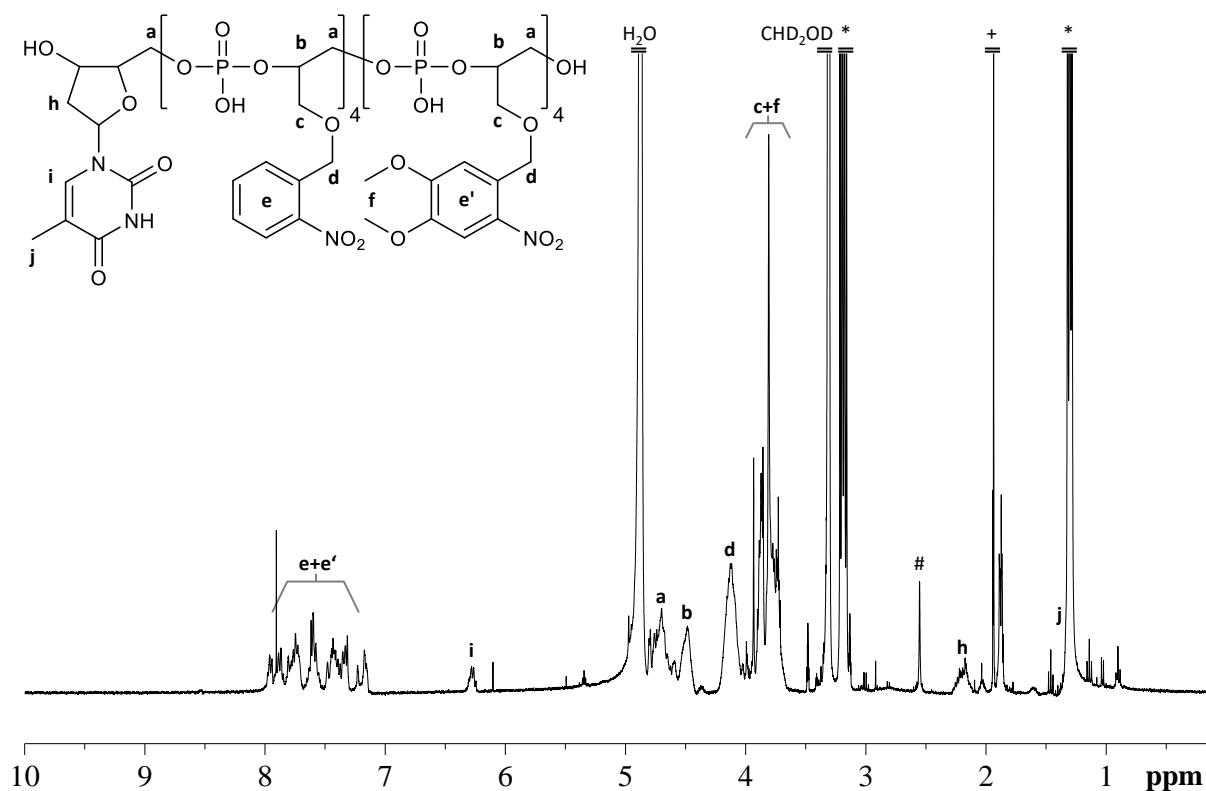
Supplementary Figure 11. ¹H NMR spectrum recorded at RT in CD₃OD for copolymer P2. The star symbols indicate signals of triethylammonium counterions. (#) Methylamine, (+) acetonitrile.



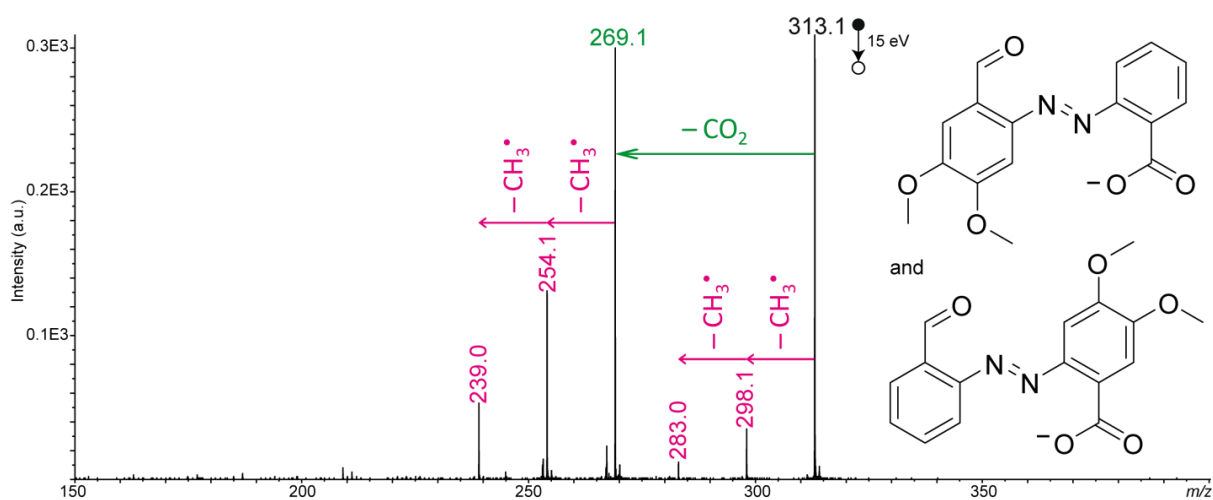
Supplementary Figure 12. ¹H NMR spectrum recorded at RT in CD₃OD for copolymer P3. The star symbols indicate signals of triethylammonium counterions. (#) Methylamine, (+) acetonitrile.



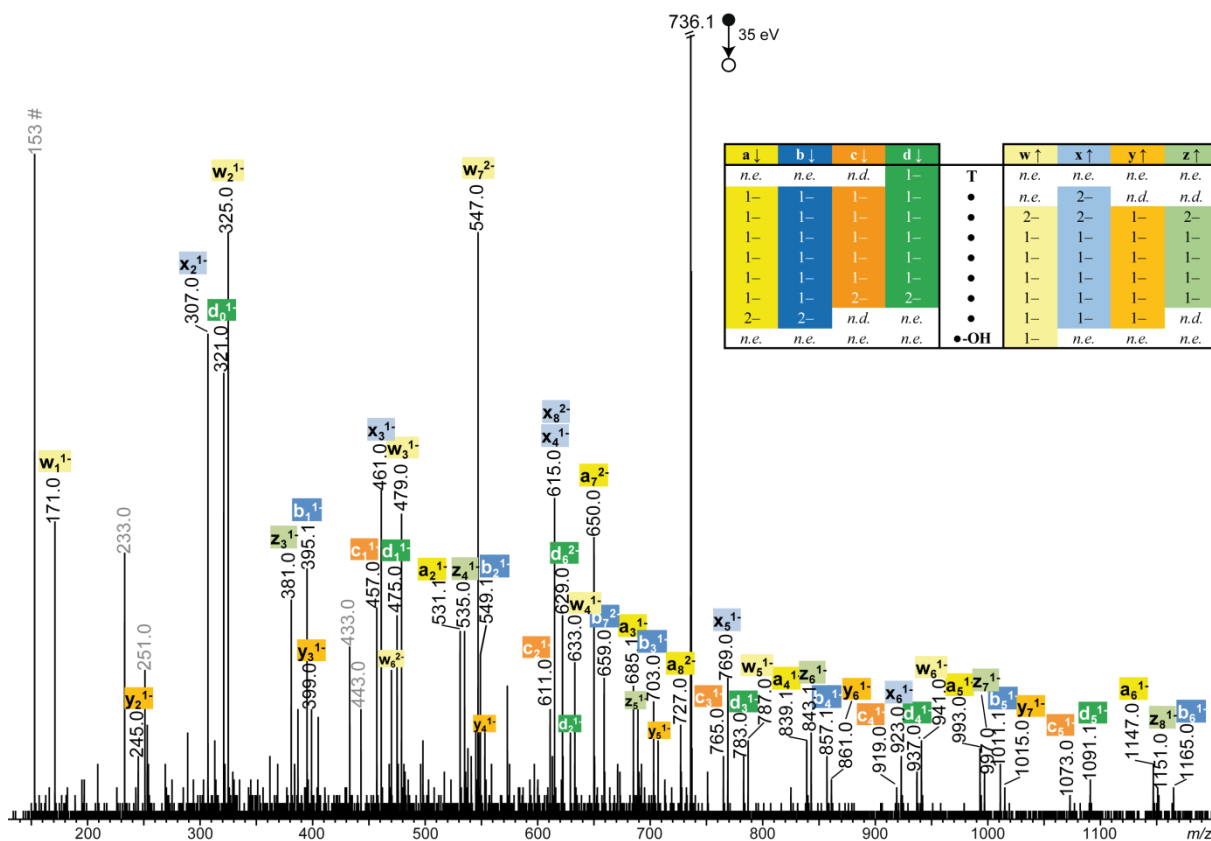
Supplementary Figure 13. ¹H NMR spectrum recorded at RT in CD₃OD for copolymer P4. The star symbols indicate signals of triethylammonium counterions. (#) Methylamine, (+) acetonitrile.



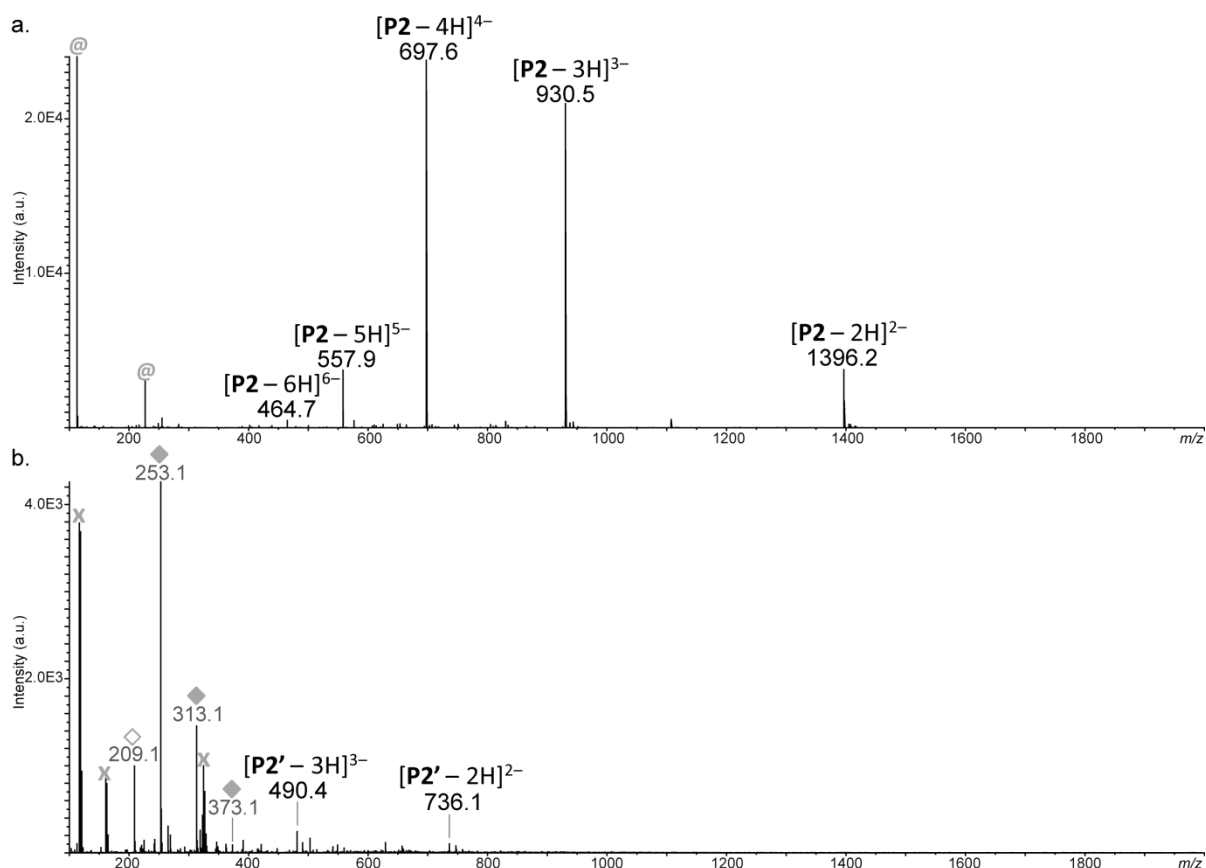
Supplementary Figure 14. ^1H NMR spectrum recorded at RT in CD_3OD for copolymer **P5**. The star symbols indicate signals of triethylammonium counterions. (#) Methylamine, (+) acetonitrile.



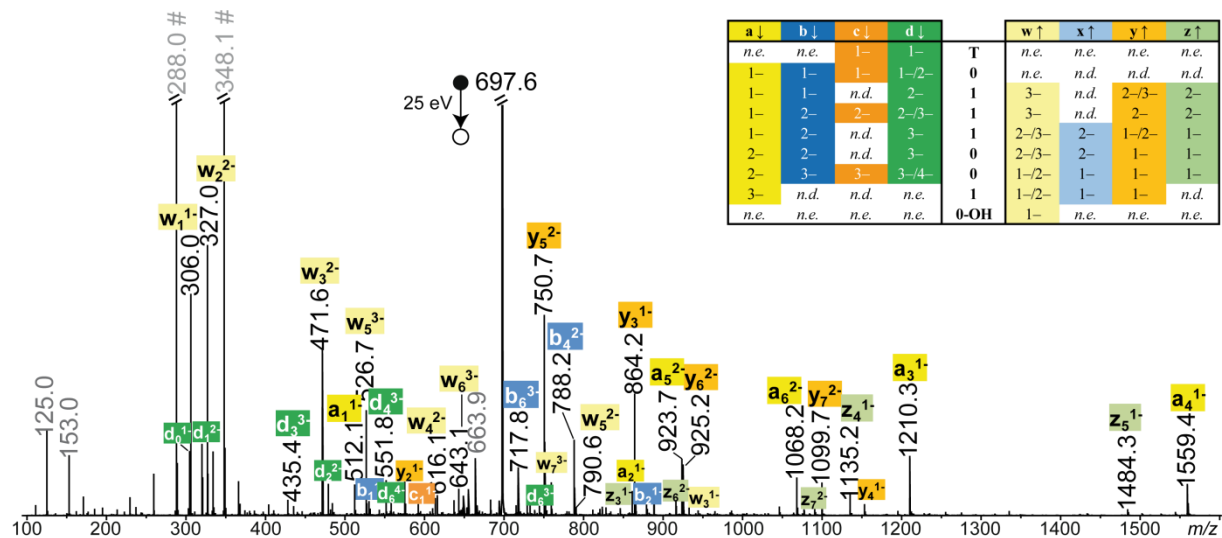
Supplementary Figure 15. MS/MS spectrum recorded for the photo-deprotection by-product observed at m/z 313.1 ($\text{C}_{16}\text{H}_{13}\text{N}_2\text{O}_5^-$, m/z_{th} 313.0830, m/z_{exp} 313.0835) after photo-irradiation of copolymer **P1**, showing that the decarboxylation product (m/z 269.1) successively eliminates two methyl radicals, consistent with the two methoxy groups in the isomeric precursors (see inset structure).



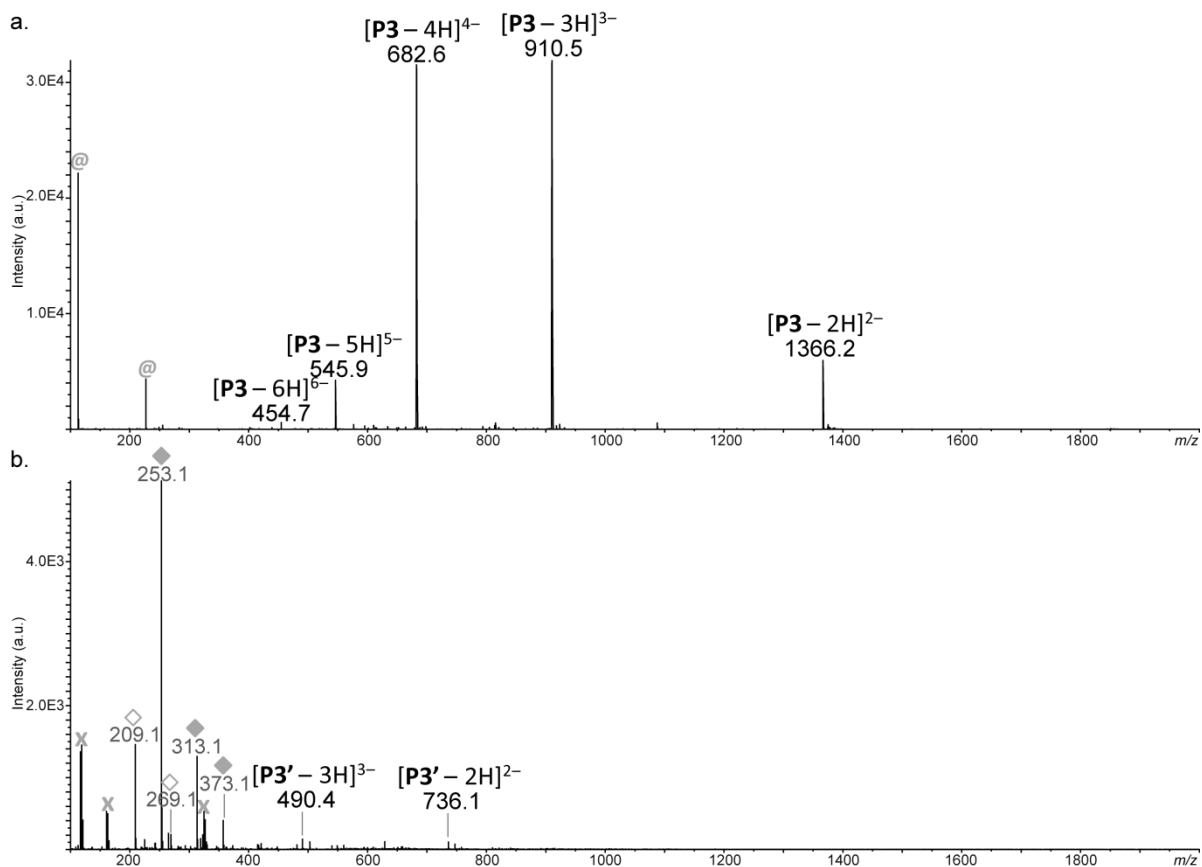
Supplementary Figure 16. MS/MS spectrum recorded for copolymer **P1'** after photo-exposure, using a 35 eV collision energy (laboratory frame) to activate the doubly deprotonated precursor at m/z 736.1. Peaks annotated in grey correspond to secondary fragments, including the deprotonated unit (m/z 153.0) designated by #. The inset table shows that most expected members of the eight fragment series are detected and evidence the monotonic sequence of **P1'**. *n.d.*: not detected. *n.e.*: not expected.



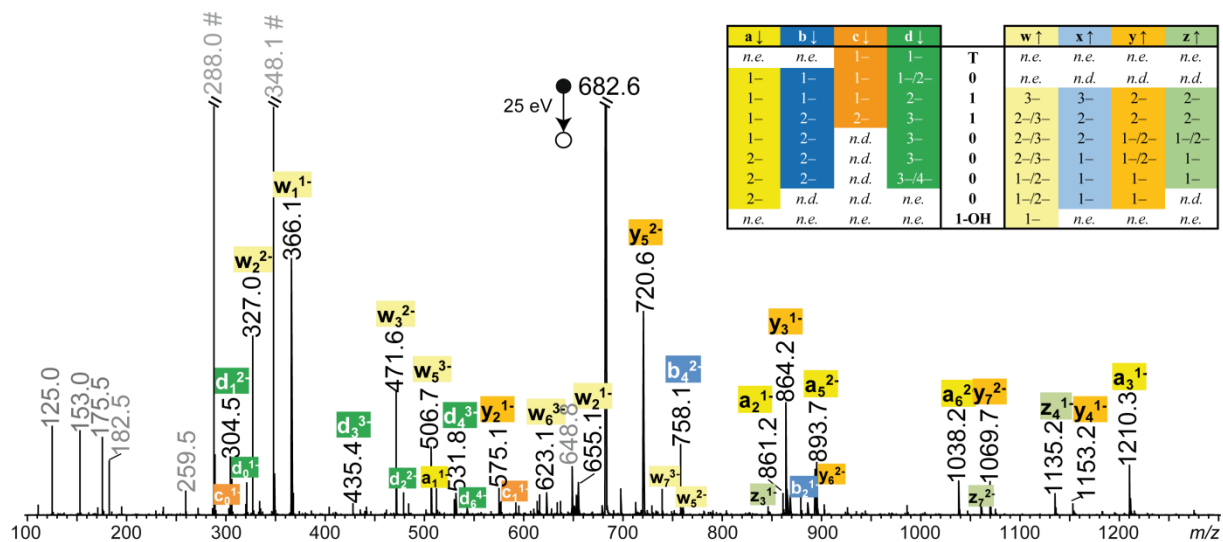
Supplementary Figure 17. ESI HRMS spectra recorded for (a) copolymer **P2** before irradiation and (b) the resulting polymer **P2'** after photo-exposure. Grey symbols designate clusters of trifluoroacetic acid (@), clusters of trichloroacetic acid (x) or photo-deprotection by-products (diamond).



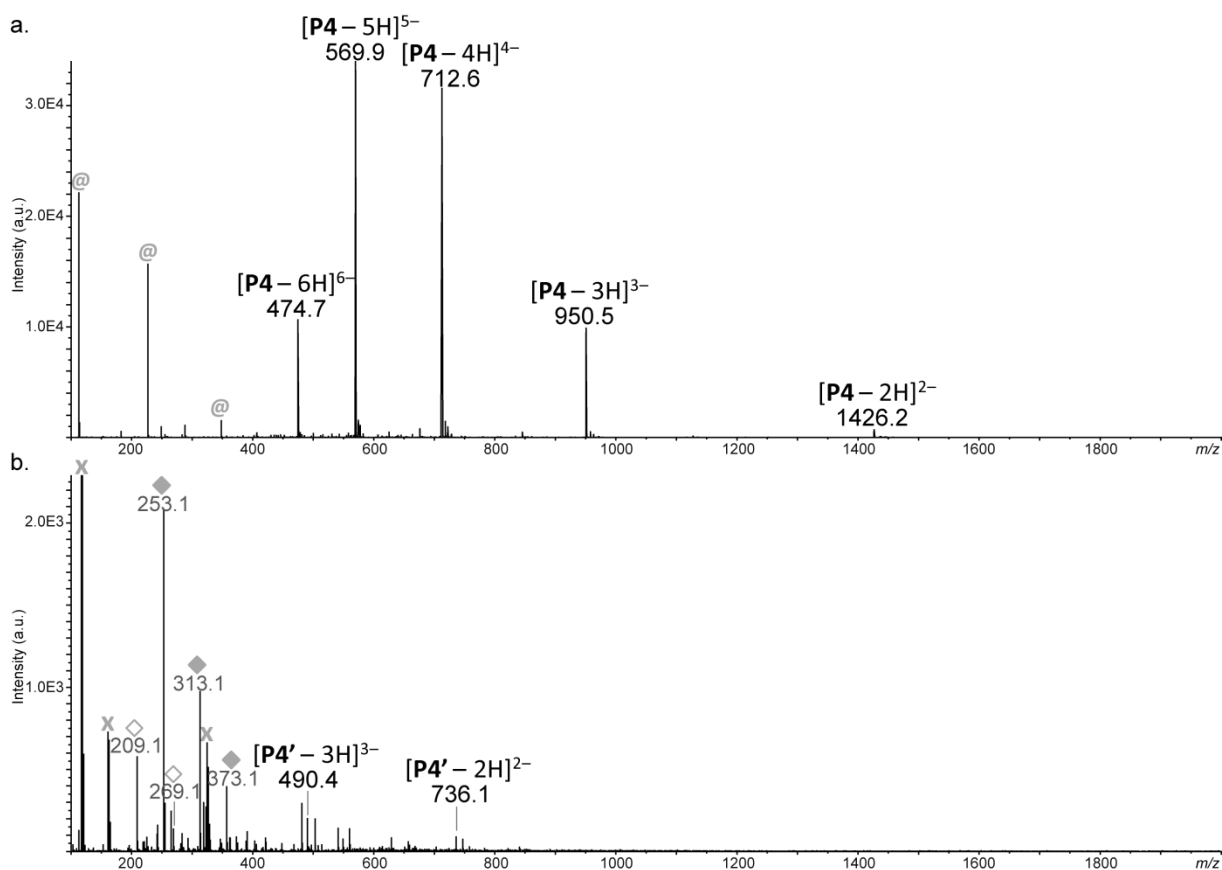
Supplementary Figure 18. MS/MS spectrum recorded for copolymer **P2** before irradiation, using a 25 eV collision energy (laboratory frame) to activate the quadruply deprotonated precursor at m/z 697.6. Peaks annotated in grey correspond to secondary fragments, including the deprotonated units, $[0 - H]^-$ at m/z 288.0 and $[1 - H]^-$ at m/z 348.1, both designated by #. Inset Table: Sequence coverage of **P2** (n.d.: not detected; n.e.: not expected). After photo-exposure, the resulting polymer **P2'** exhibits the same MS/MS spectrum as **P1'** in Supplementary Figure 16.



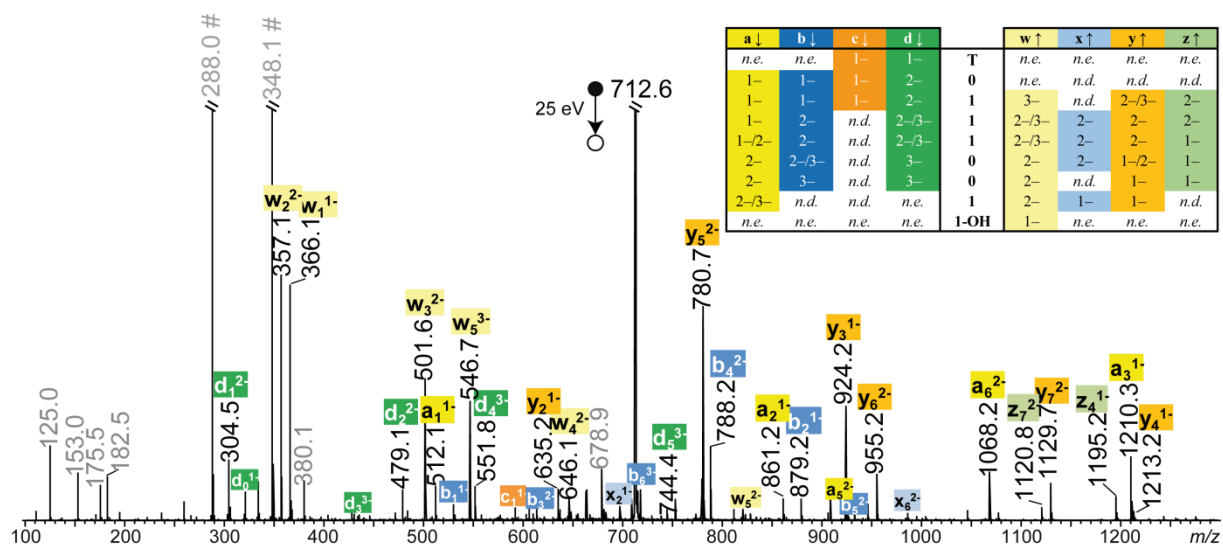
Supplementary Figure 19. ESI HRMS spectra recorded for (a) copolymer **P3** before irradiation and (b) the resulting polymer **P3'** after photo-exposure. Grey symbols designate clusters of trifluoroacetic acid (@), clusters of trichloroacetic acid (x) or photo-deprotection by-products (diamond).



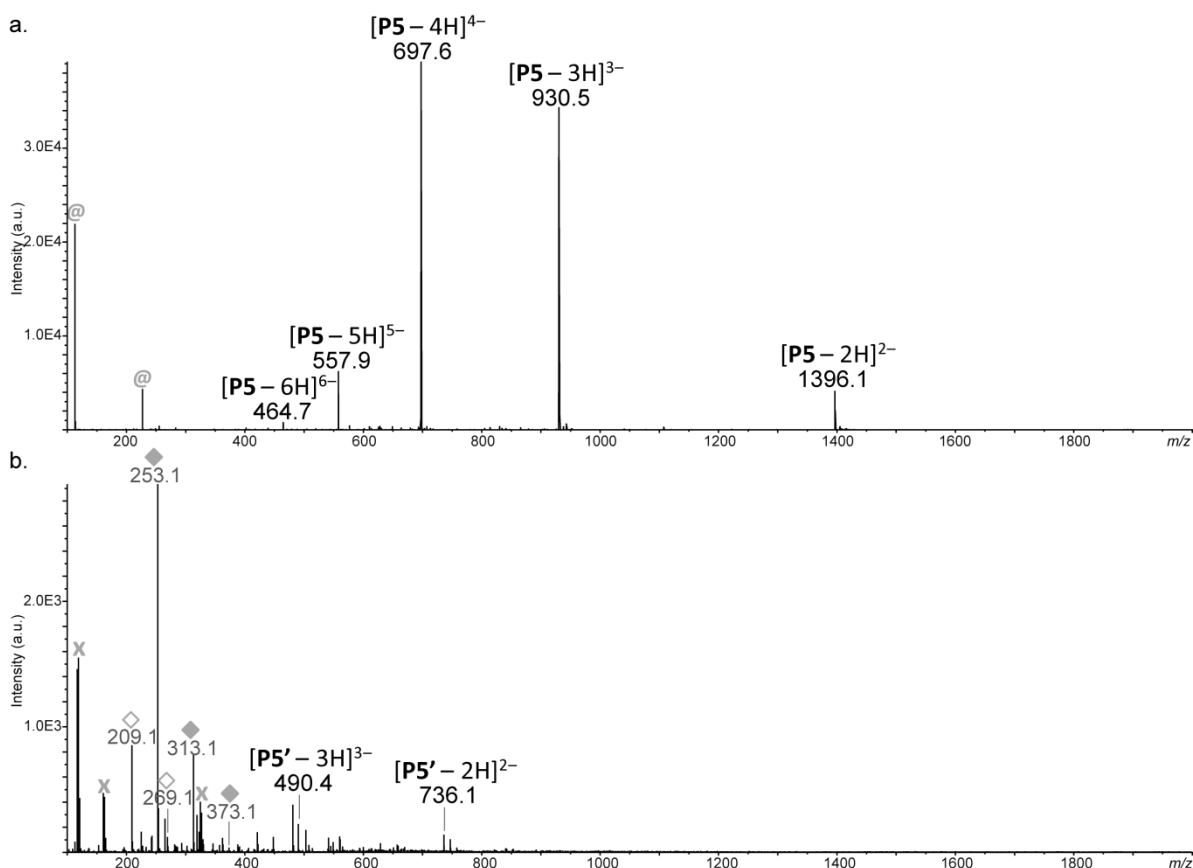
Supplementary Figure 20. MS/MS spectrum recorded for copolymer **P3** before irradiation, using a 25 eV collision energy (laboratory frame) to activate the quadruply deprotonated precursor at m/z 682.6. Peaks annotated in grey correspond to secondary fragments, including the deprotonated units, $[0-H]^-$ at m/z 288.0 and $[1-H]^-$ at m/z 348.1, both designated by #. Inset Table: Sequence coverage of **P3** (n.d.: not detected; n.e.: not expected). After photo-exposure, the resulting polymer **P3'** exhibits the same MS/MS spectrum as **P1'** in Supplementary Figure 16.



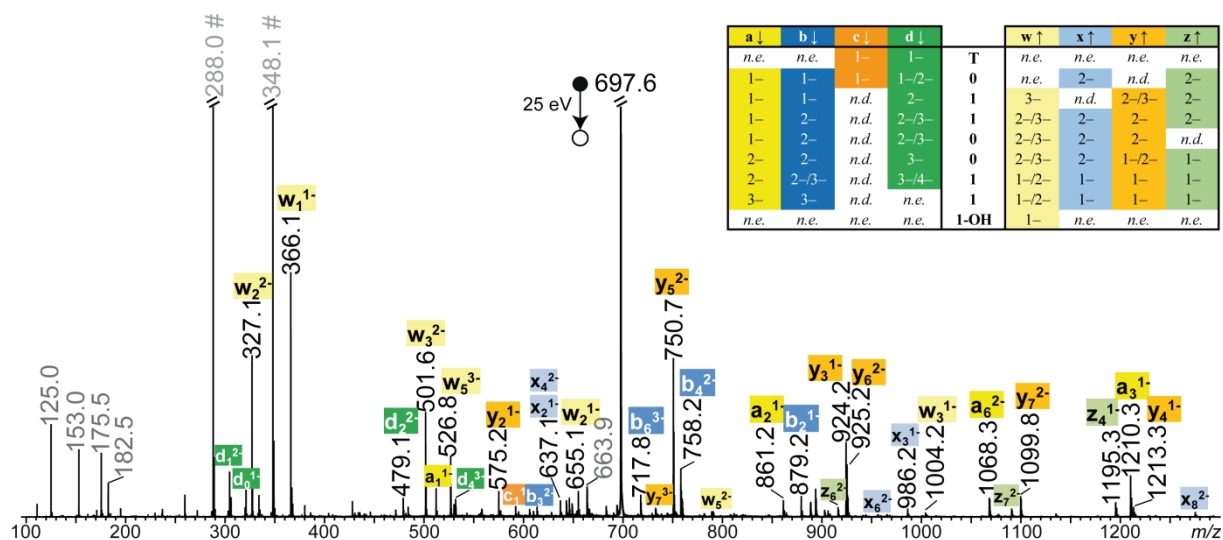
Supplementary Figure 21. ESI HRMS spectra recorded for (a) copolymer **P4** before irradiation and (b) the resulting polymer **P4'** after photo-exposure. Grey symbols designate clusters of trifluoroacetic acid (@), clusters of trichloroacetic acid (x) or photo-deprotection by-products (diamond).



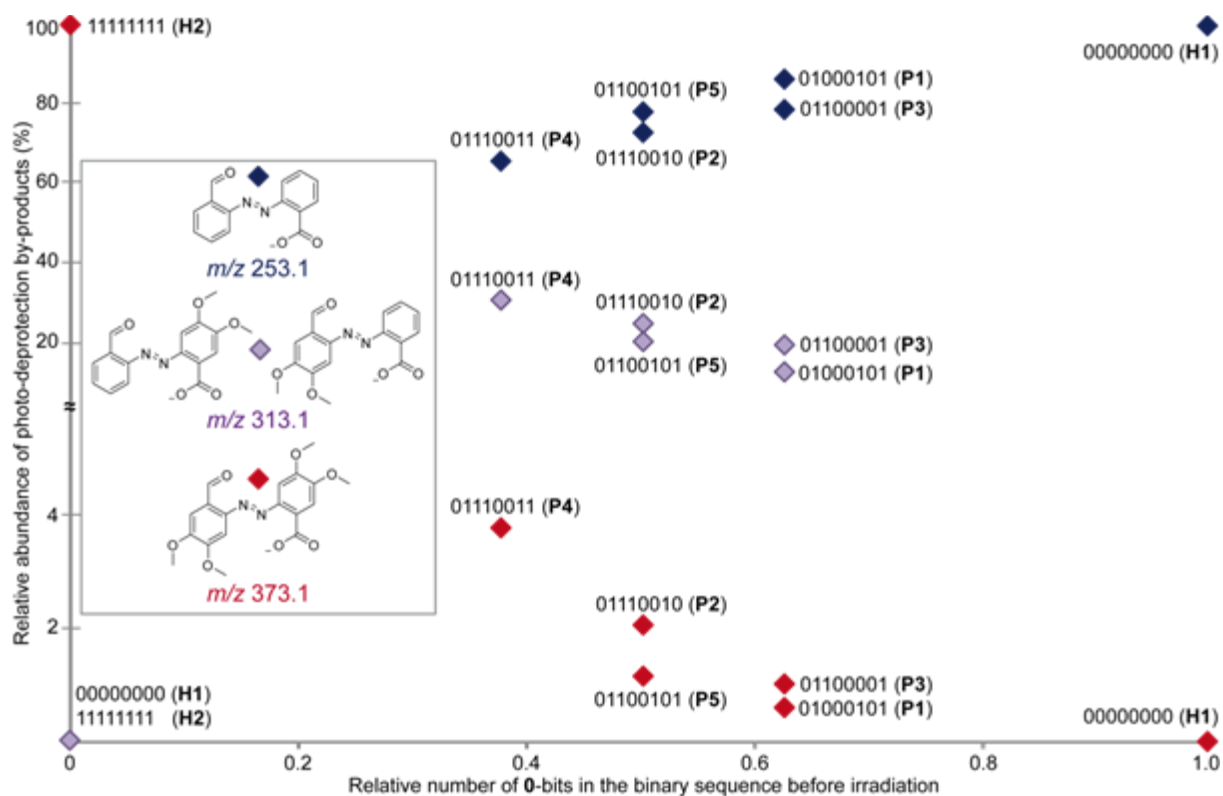
Supplementary Figure 22. MS/MS spectrum recorded for copolymer **P4** before irradiation, using a 25 eV collision energy (laboratory frame) to activate the quadruply deprotonated precursor at m/z 712.6. Peaks annotated in grey correspond to secondary fragments, including the deprotonated units, $[0 - H]^-$ at m/z 288.0 and $[1 - H]^-$ at m/z 348.1, both designated by #. Inset Table: Sequence coverage of **P4** (n.d.: not detected; n.e.: not expected). After photo-exposure, the resulting polymer **P4'** exhibits the same MS/MS spectrum as **P1'** in Supplementary Figure 16.



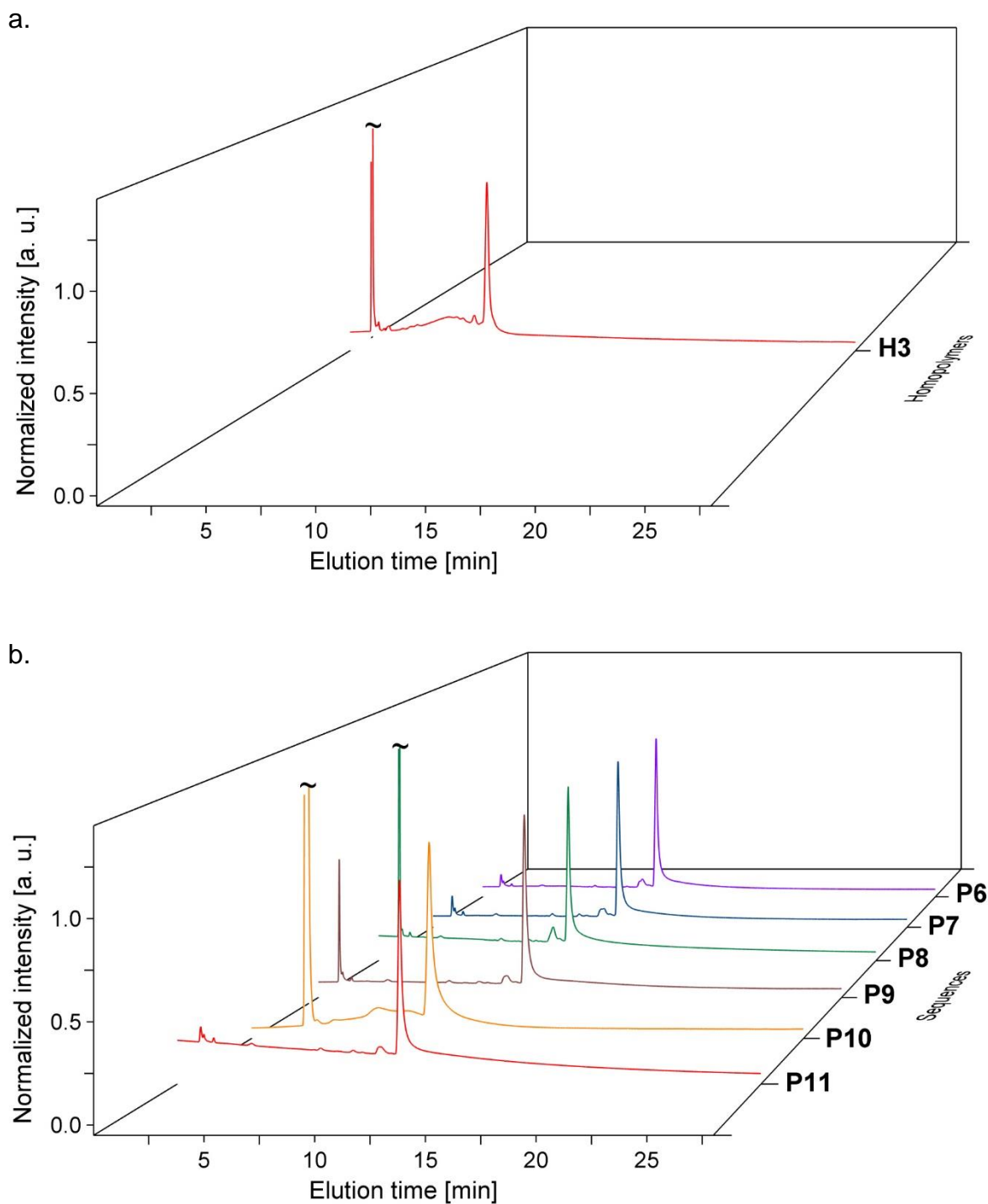
Supplementary Figure 23. ESI HRMS spectra recorded for (a) copolymer **P5** before irradiation and (b) the resulting polymer **P5'** after photo-exposure. Grey symbols designate clusters of trifluoroacetic acid (@), clusters of trichloroacetic acid (x) or photo-deprotection by-products (diamond).



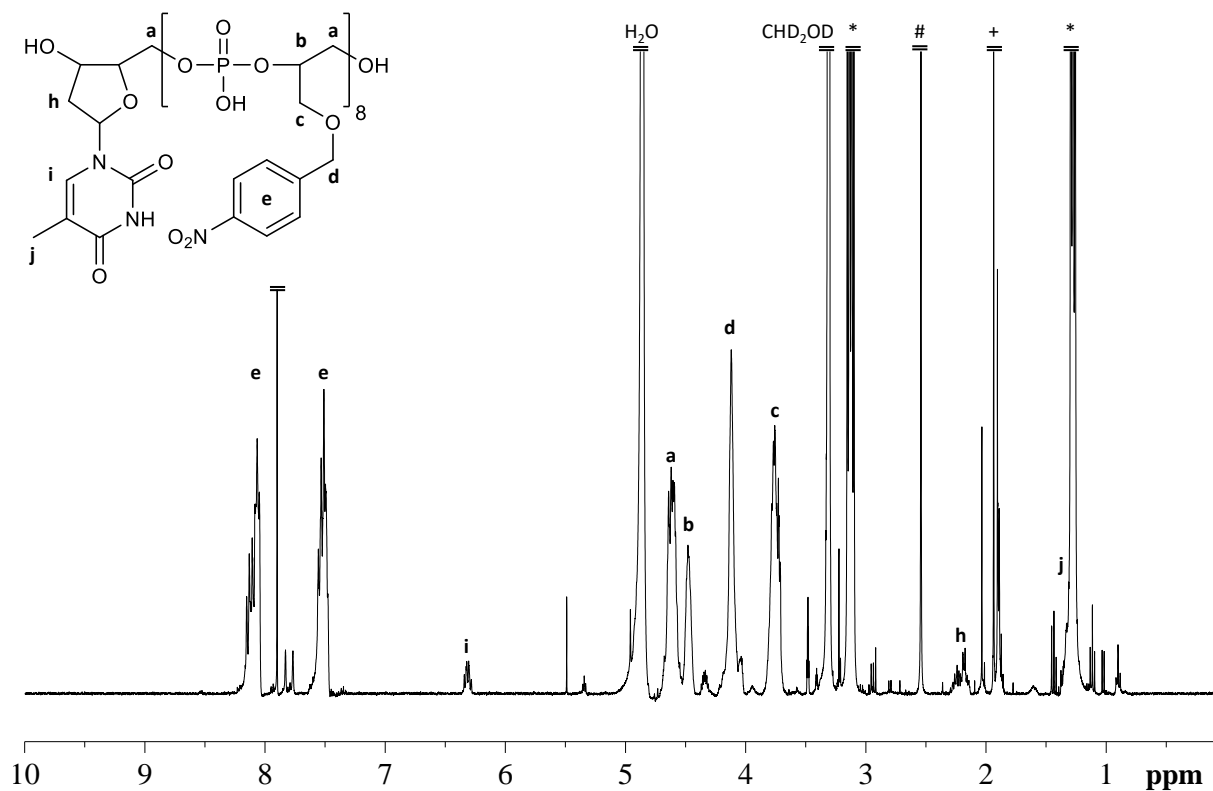
Supplementary Figure 24. MS/MS spectrum recorded for copolymer **P5** before irradiation, using a 25 eV collision energy (laboratory frame) to activate the quadruply deprotonated precursor at m/z 697.6. Peaks annotated in grey correspond to secondary fragments, including the deprotonated units, [0-H]⁻ at m/z 288.0 and [1-H]⁻ at m/z 348.1, both designated by #. Inset Table: Sequence coverage of **P5** (n.d.: not detected; n.e.: not expected). After photo-exposure, the resulting polymer **P5'** exhibits the same MS/MS spectrum as **P1'** in Supplementary Figure 16.



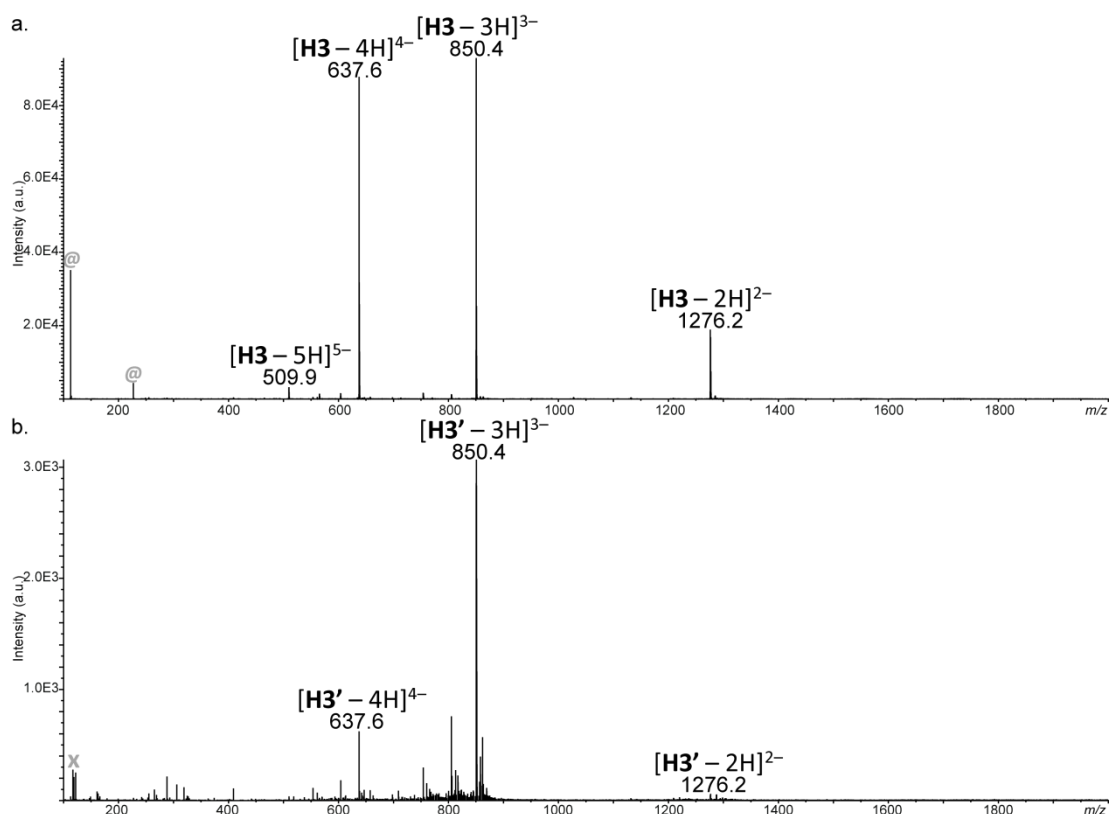
Supplementary Figure 25. Relative abundance of photolysis by-products (structure shown in inset) as a function of 0/1 comonomer composition of the polymer before photo-irradiation. Each data point is annotated by the sequence of the corresponding polymer before irradiation. The relative amount of the homodimer detected at m/z 253.1 increases with the fraction of 0-bits in the original sequence. Similarly, the relative abundance of the homodimer detected at m/z 373.1 increase with the fraction of 1-bits (i.e., decreasing fraction of 0-bits) in the original sequence. Consistent with the decreasing amount of photocleaved veratryl units in the irradiated solution, the relative intensity of the m/z 313.1 signal, assigned to a heterodimer, decreased as the fraction of 0-bits increased in the original sequence.



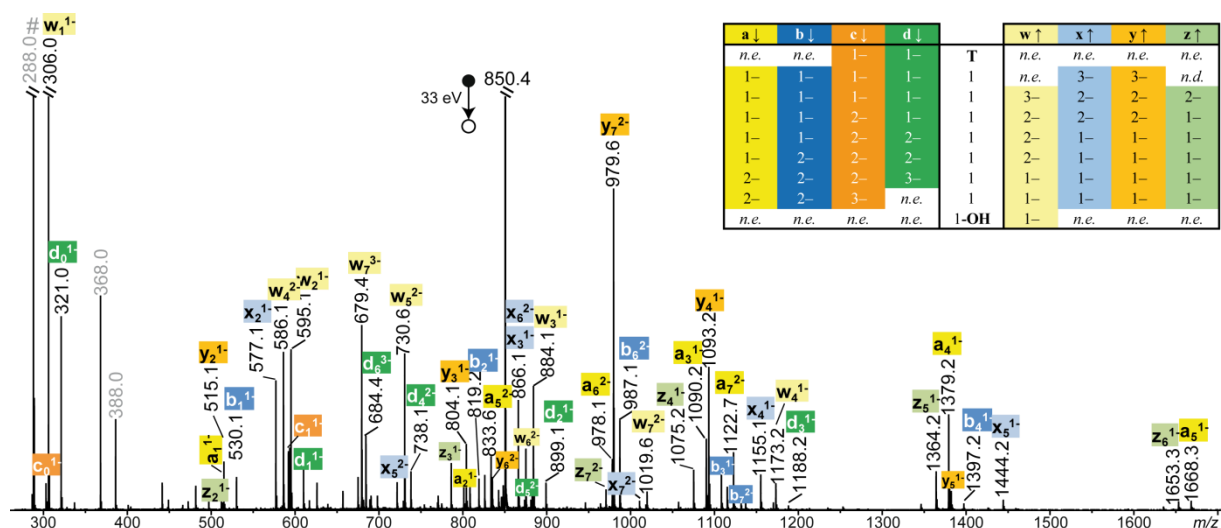
Supplementary Figure 26. HPLC traces measured for (a) homopolymers **H3** and (b) copolymers **P6-P11**. The chromatograms are recorded at $\lambda = 260$ nm. Experimental conditions: phase A: 10 % MeCN 20 % 2M NH_3 in water, phase B: 2.5 M NaCl in water; gradient: 0-3 min 5 % B, 3-23 min 5 % B-30 % B, 23-28 min 30 % B, 28-35 min 30% \rightarrow 5 % B; flow rate: 1 mL \cdot min $^{-1}$.



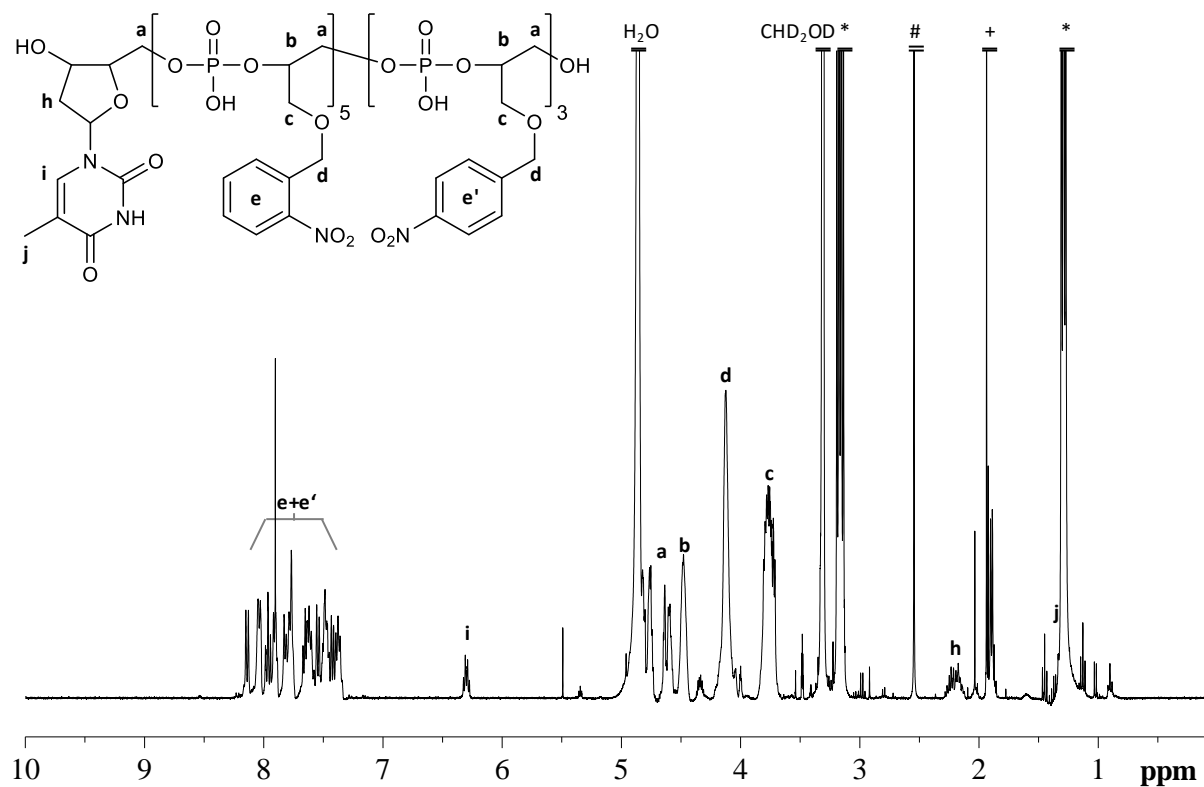
Supplementary Figure 27. ¹H NMR spectrum recorded at RT in CD₃OD for homopolymer **H3**. The star symbols indicate signals of triethylammonium counterions. (#) Methylamine, (+) acetonitrile.



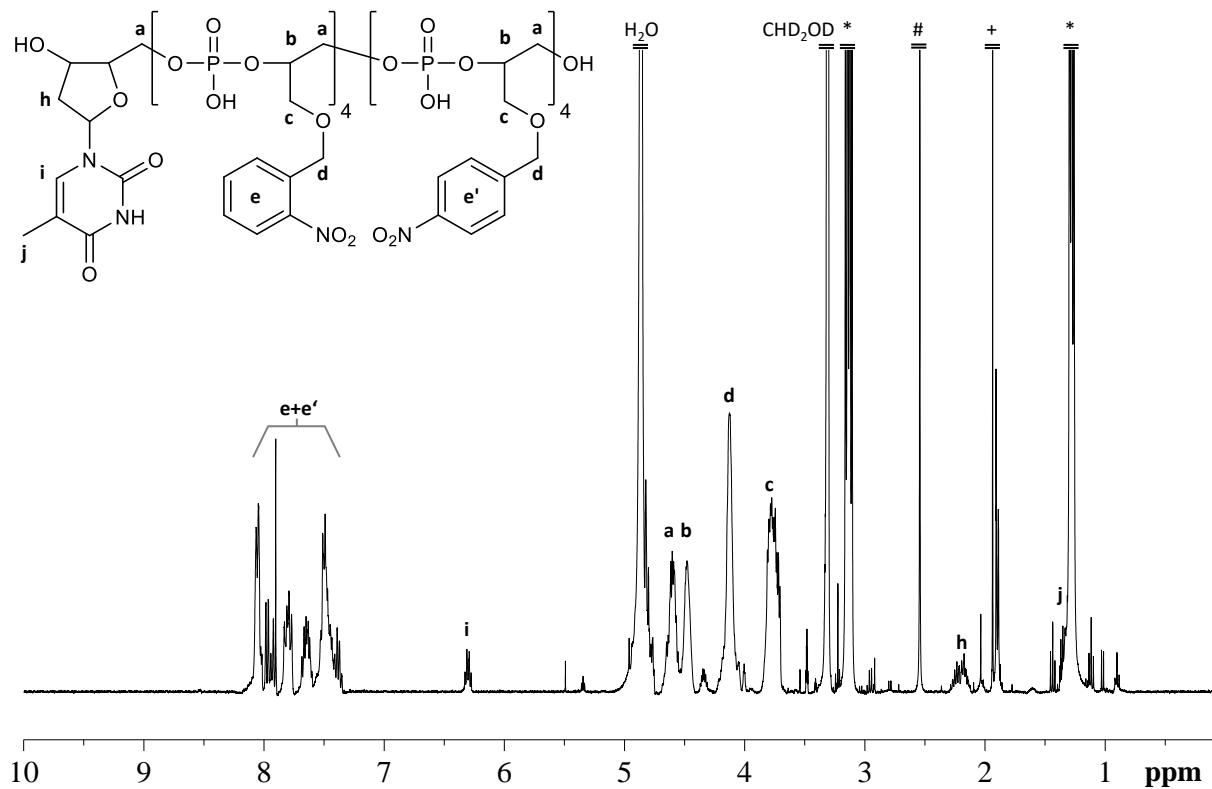
Supplementary Figure 28. ESI HRMS spectra recorded for (a) homopolymer **H3** before irradiation and (b) the resulting polymer **H3'** after photo-exposure. Grey symbols designate clusters of trifluoroacetic acid (@) and clusters of trichloroacetic acid (x).



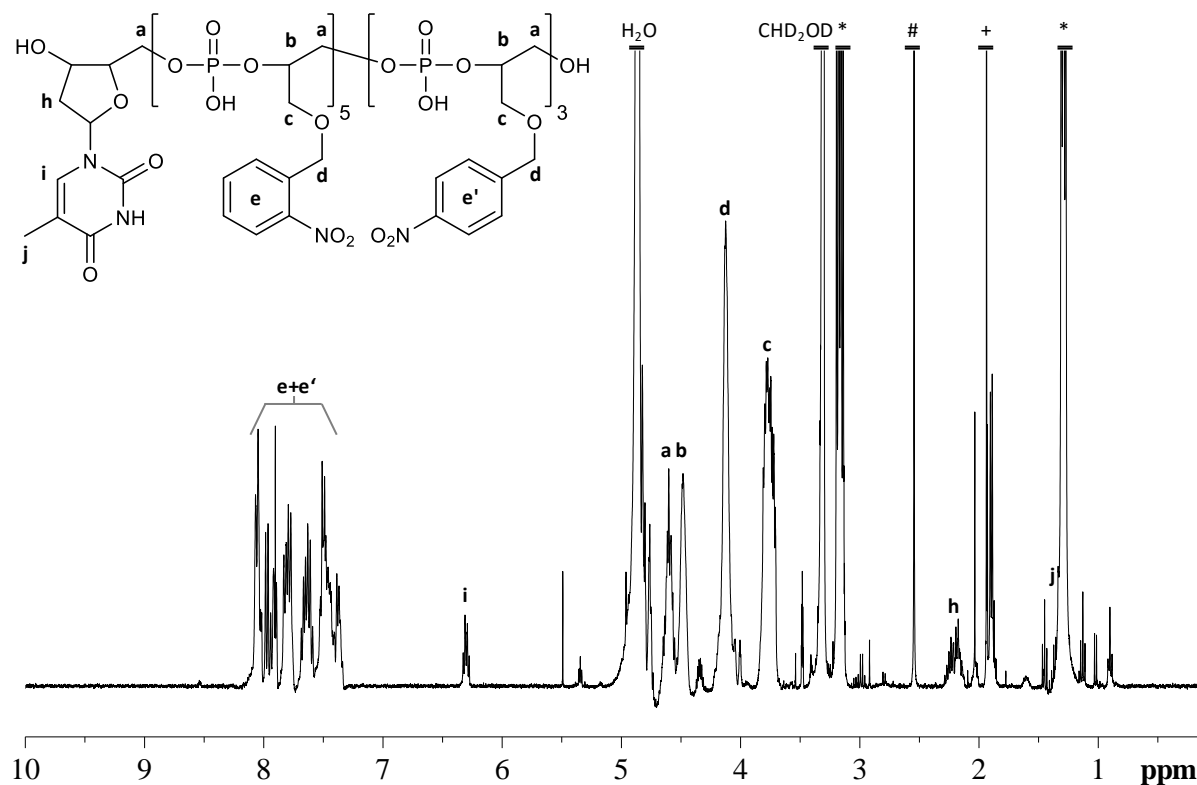
Supplementary Figure 29. MS/MS spectrum recorded for homopolymer **H3** before photo-exposure, using a 33 eV collision energy (laboratory frame) to activate the triply deprotonated precursor at m/z 850.4. Peaks annotated in grey correspond to secondary fragments, including the deprotonated unit (m/z 288.0) designated by #. The inset table shows that most expected members of the eight fragment series are detected and evidence the monotonic sequence of **H3**. *n.d.*: not detected. *n.e.*: not expected.



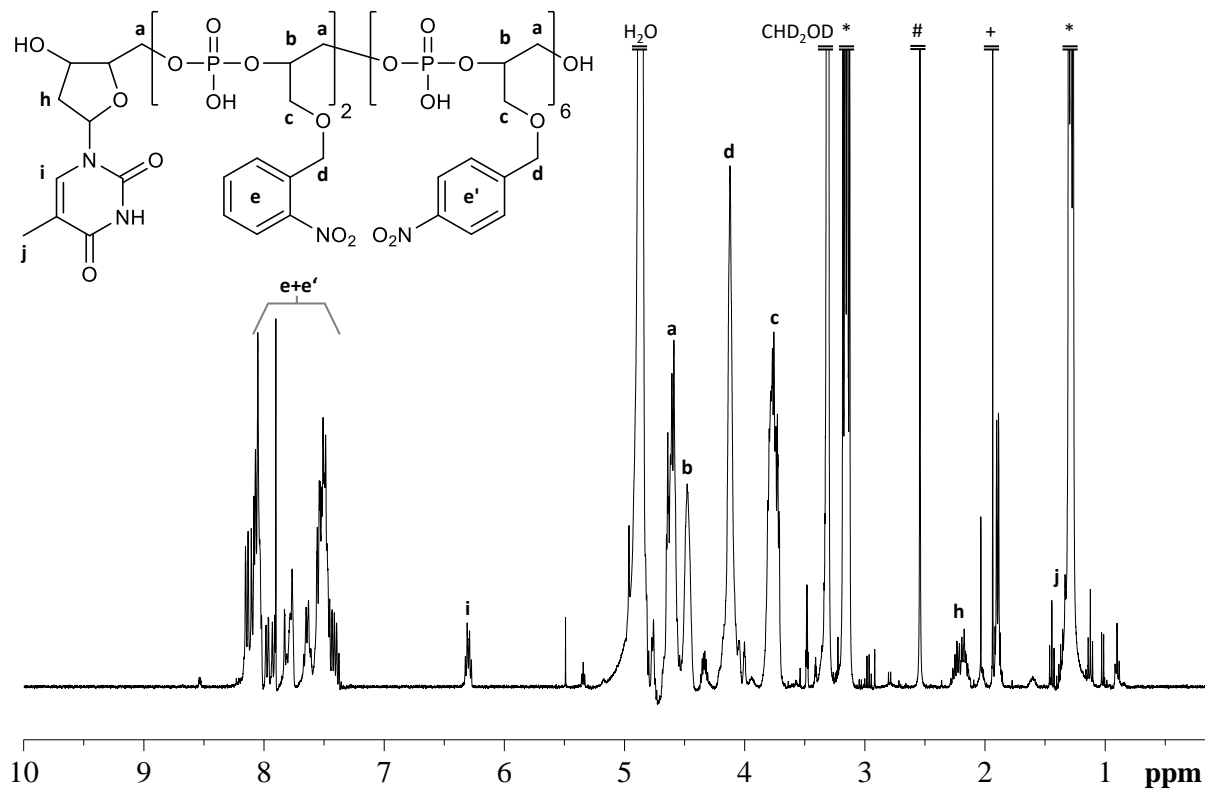
Supplementary Figure 30. ¹H NMR spectrum recorded at RT in CD₃OD for copolymer **P6**. The star symbols indicate signals of triethylammonium counterions. (#) Methylamine, (+) acetonitrile.



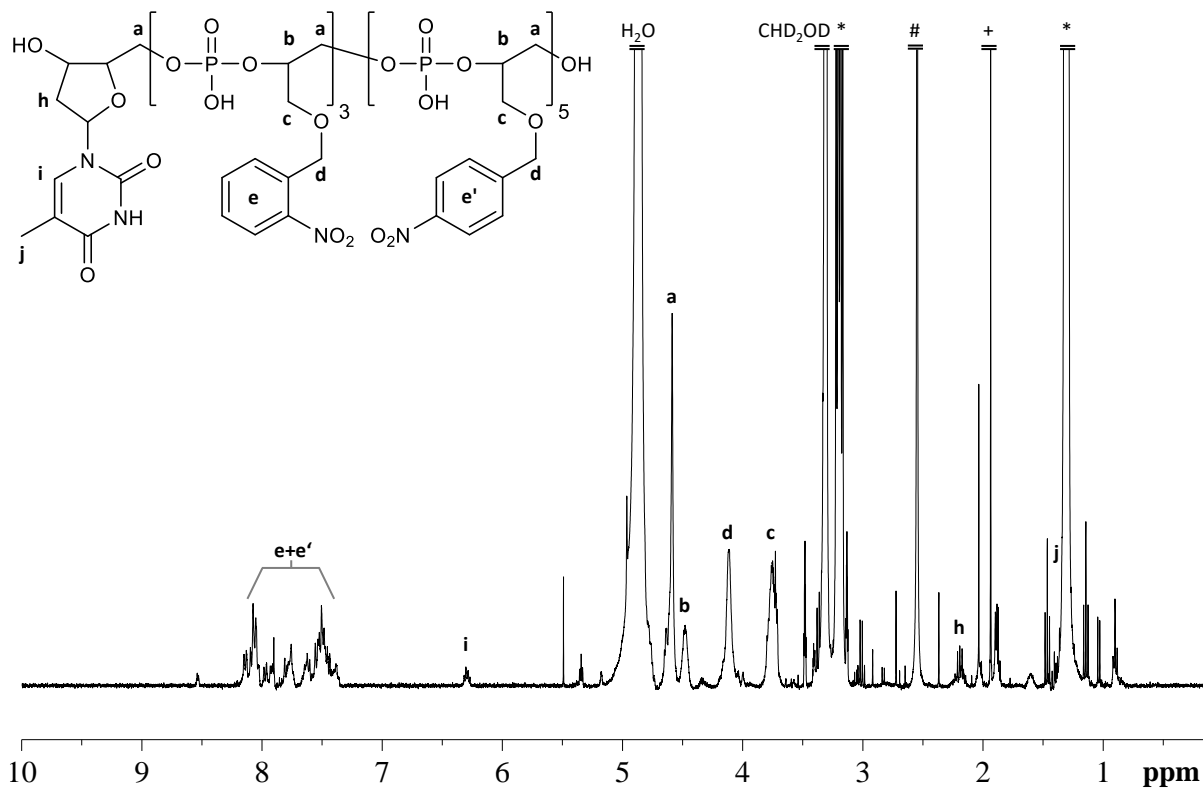
Supplementary Figure 31. ¹H NMR spectrum recorded at RT in CD₃OD for copolymer **P7**. The star symbols indicate signals of triethylammonium counterions. (#) Methylamine, (+) acetonitrile.



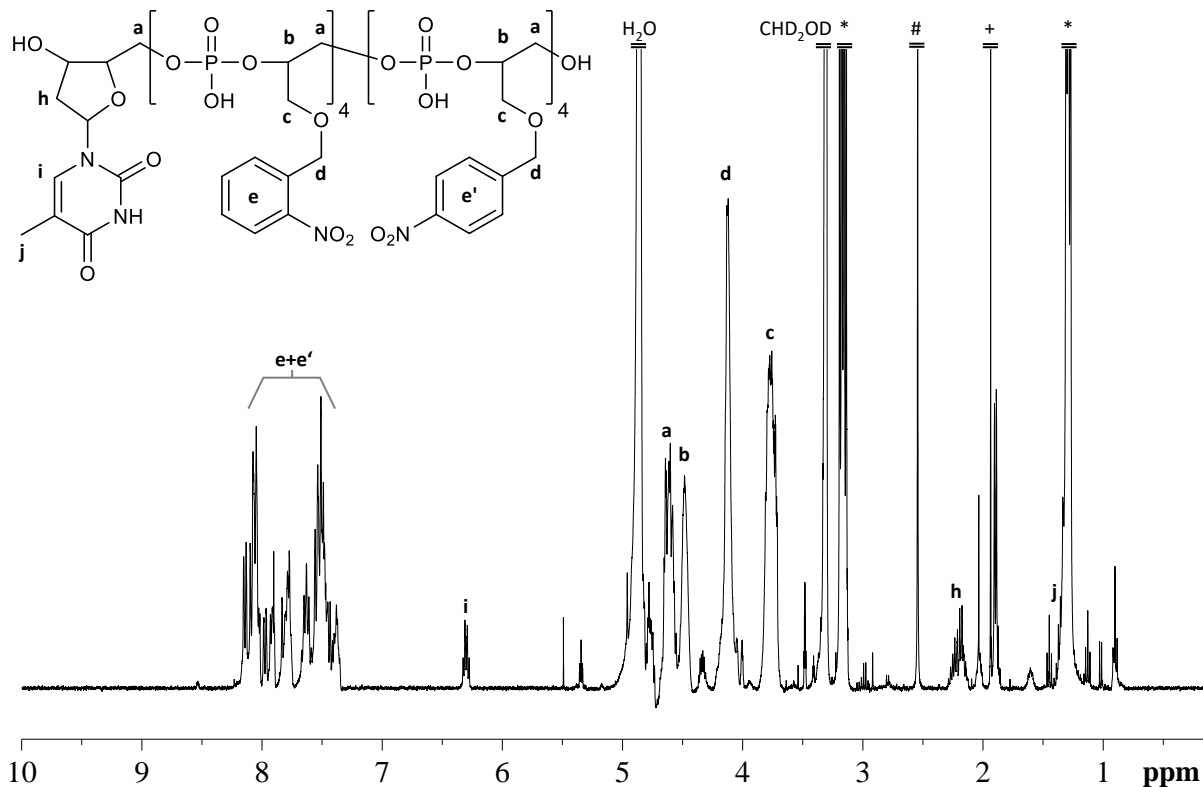
Supplementary Figure 32. ^1H NMR spectrum recorded at RT in CD_3OD for copolymer **P8**. The star symbols indicate signals of triethylammonium counterions. (#) Methylamine, (+) acetonitrile.



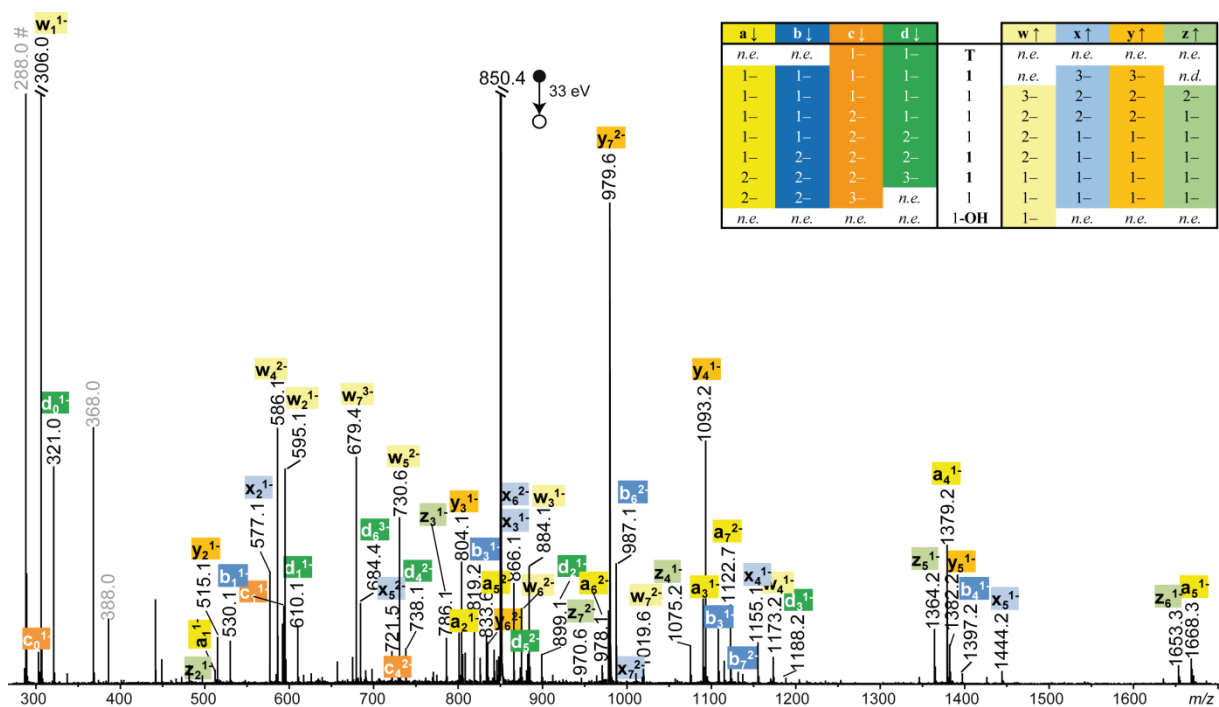
Supplementary Figure 33. ^1H NMR spectrum recorded at RT in CD_3OD for copolymer **P9**. The star symbols indicate signals of triethylammonium counterions. (#) Methylamine, (+) acetonitrile.



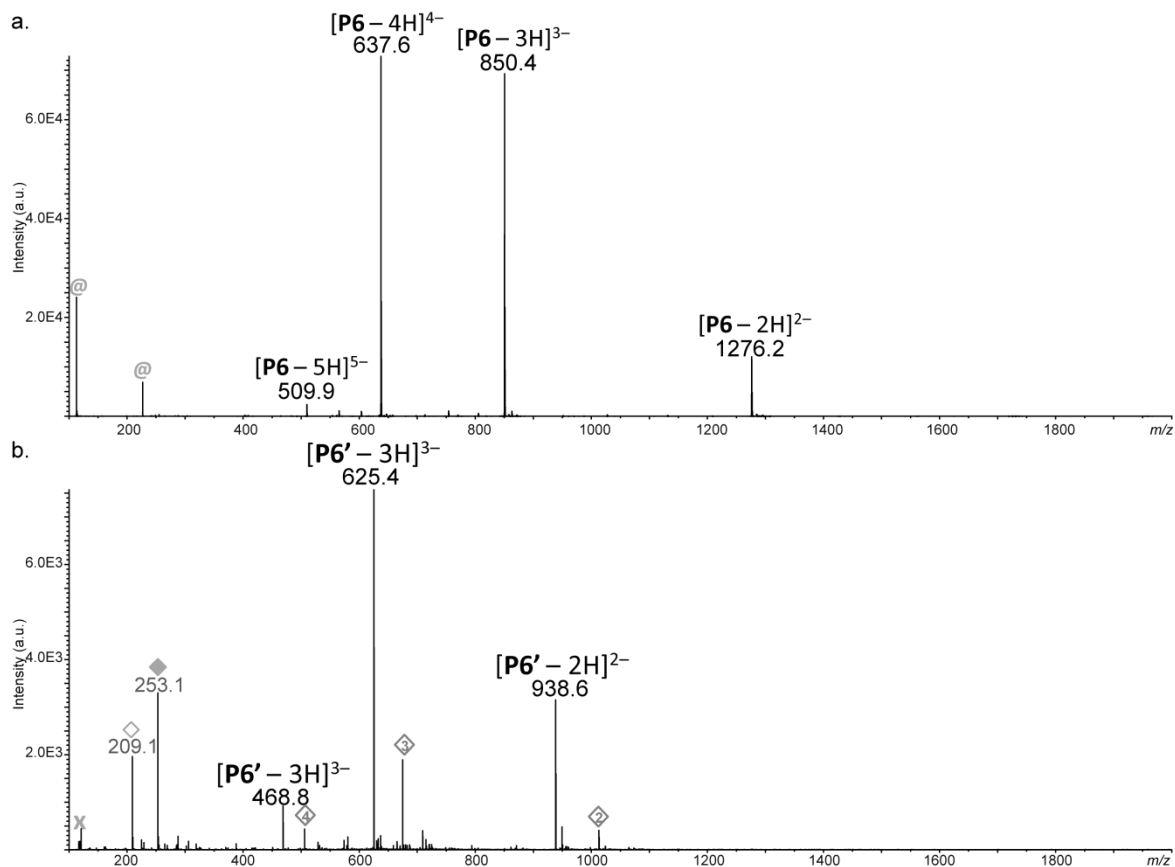
Supplementary Figure 34. ¹H NMR spectrum recorded at RT CD₃OD for copolymer **P10**. The star symbols indicate signals of triethylammonium counterions. (#) Methylamine, (+) acetonitrile.



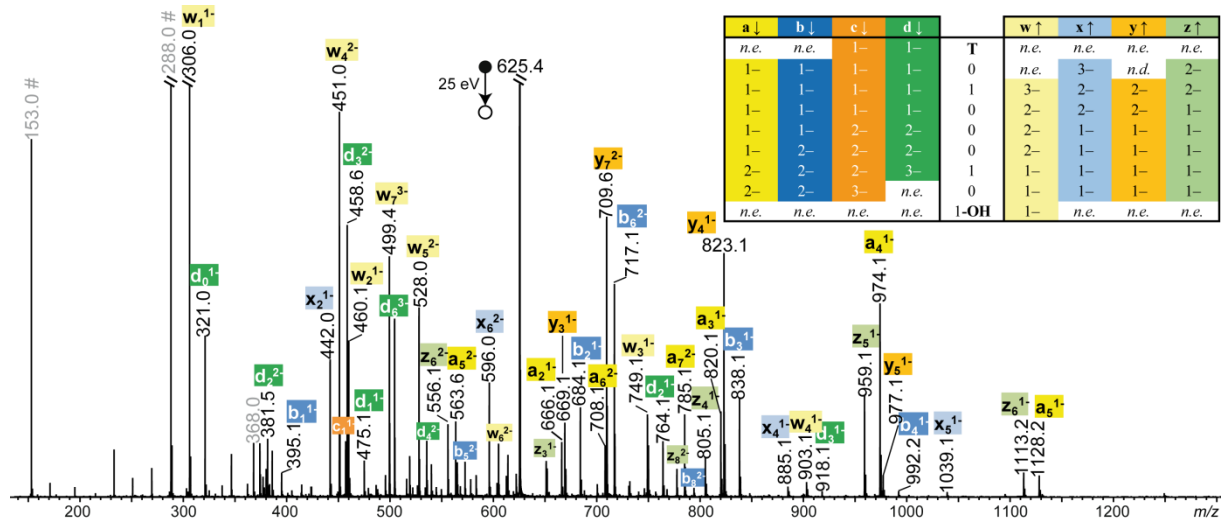
Supplementary Figure 35. ¹H NMR spectrum recorded at RT CD₃OD for copolymer **P11**. The star symbols indicate signals of triethylammonium counterions. (#) Methylamine, (+) acetonitrile.



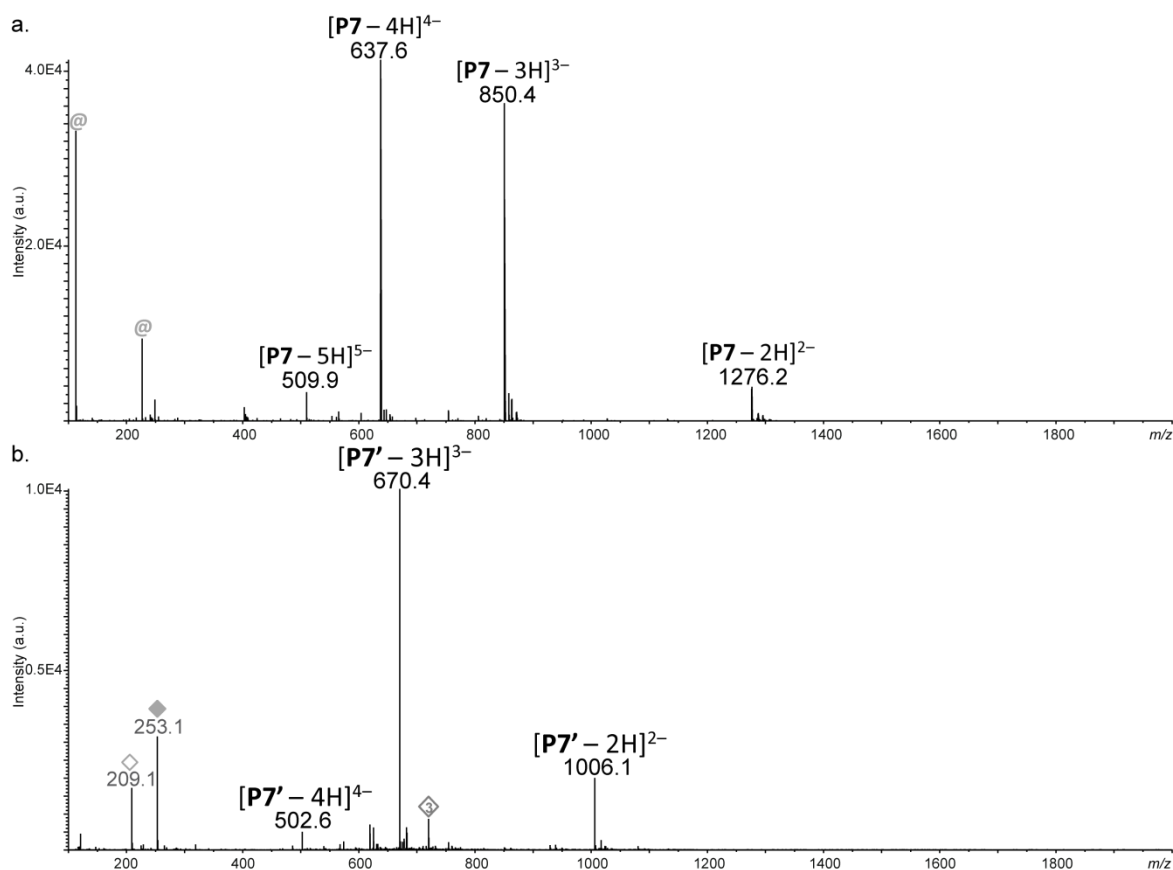
Supplementary Figure 36. MS/MS spectrum recorded for copolymer **P10** before irradiation, using a 33 eV collision energy (laboratory frame) to activate the triply deprotonated precursor at m/z 850.4. Peaks annotated in grey correspond to secondary fragments, including deprotonated units (both at m/z 288.0) designated by #. The inset table shows that all (but one) expected members of the eight fragment series are detected and evidence the monotonic sequence of **P10** (*n.d.*: not detected; *n.e.*: not expected).



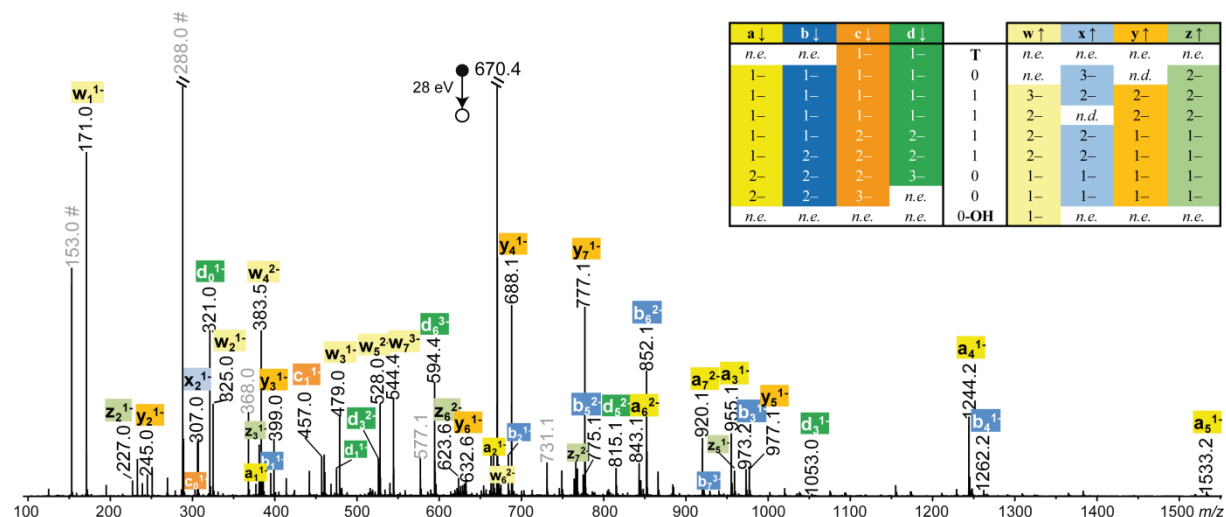
Supplementary Figure 37. ESI HRMS spectra recorded for (a) copolymer **P6** before irradiation and (b) the resulting polymer **P6'** after photo-exposure. Grey symbols designate clusters of trifluoroacetic acid (@), clusters of trichloroacetic acid (x) or photo-deprotection by-products (diamonds).



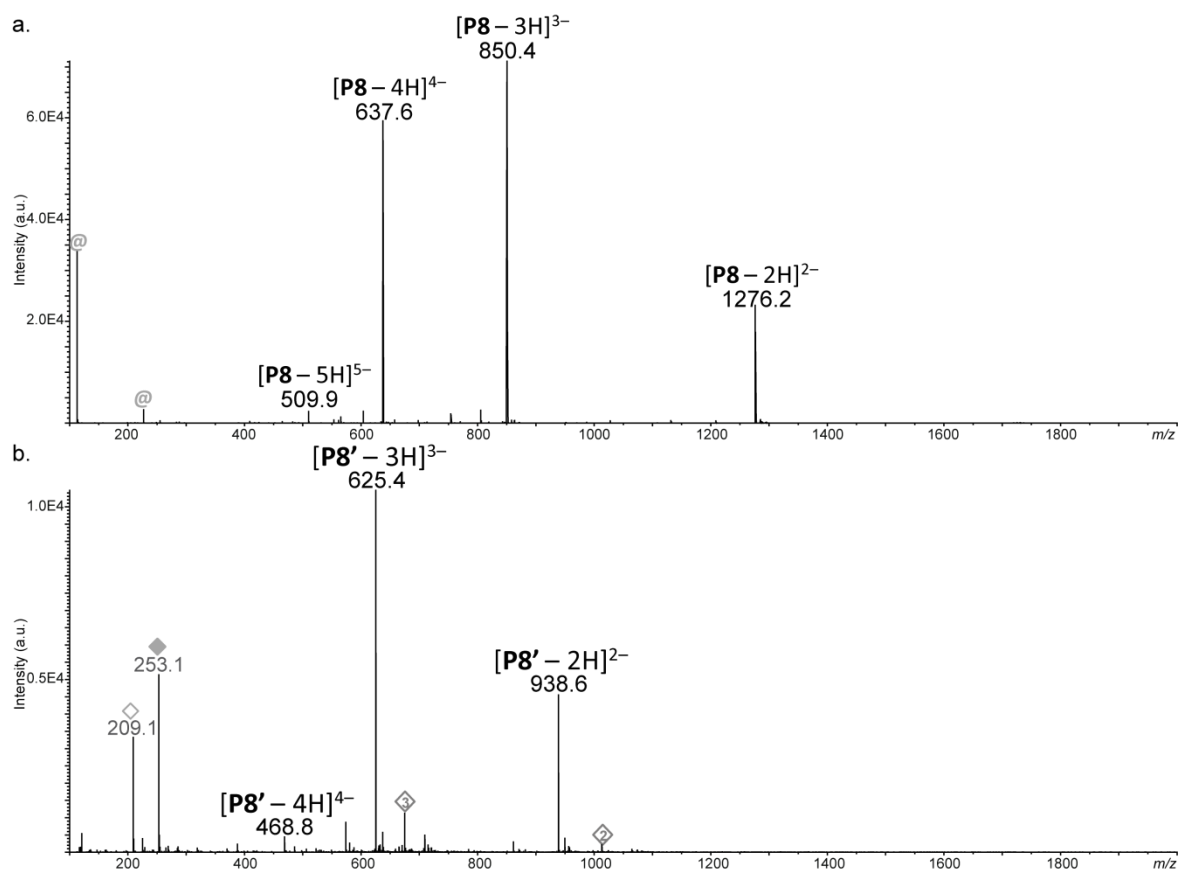
Supplementary Figure 38. MS/MS spectrum recorded for copolymer **P6'** obtained after irradiation of **P6**, using a 25 eV collision energy (laboratory frame) to activate the triply deprotonated precursor at m/z 625.4. Peaks annotated in grey correspond to secondary fragments, including the deprotonated units, $[0-H]^-$ at m/z 153.0 and $[1-H]^-$ at m/z 288.0, both designated by #. Inset Table: Sequence coverage of **P6'** (n.d.: not detected; n.e.: not expected). Before photo-exposure, copolymer **P6** exhibits the same MS/MS spectrum as **P10** in Supplementary Figure 35.



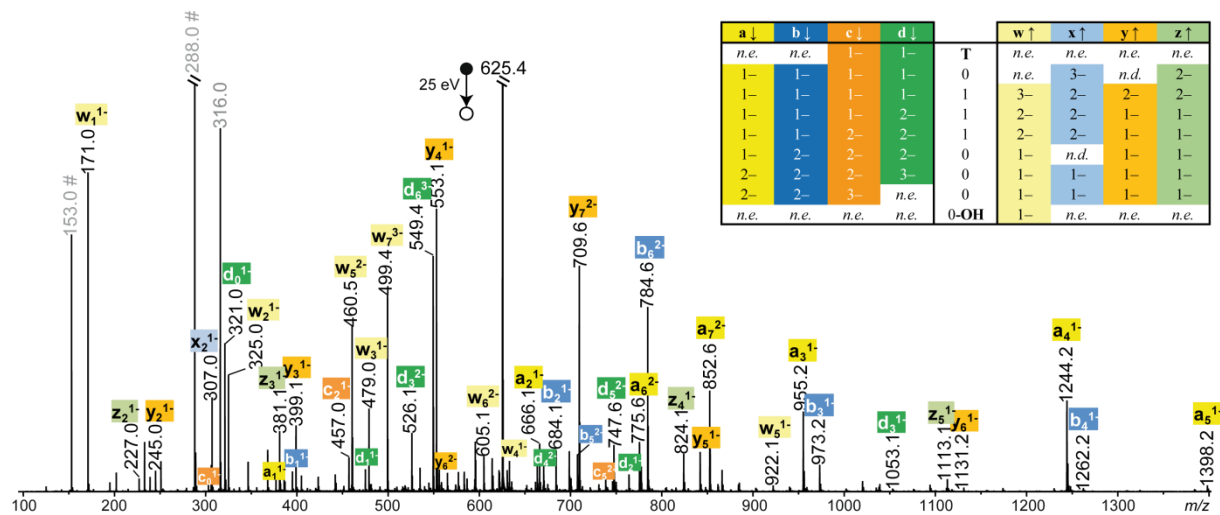
Supplementary Figure 39. ESI HRMS spectra recorded for (a) copolymer **P7** before irradiation and (b) the resulting polymer **P7'** after photo-exposure. Grey symbols designate clusters of trifluoroacetic acid (@) or photo-deprotection by-products (diamonds).



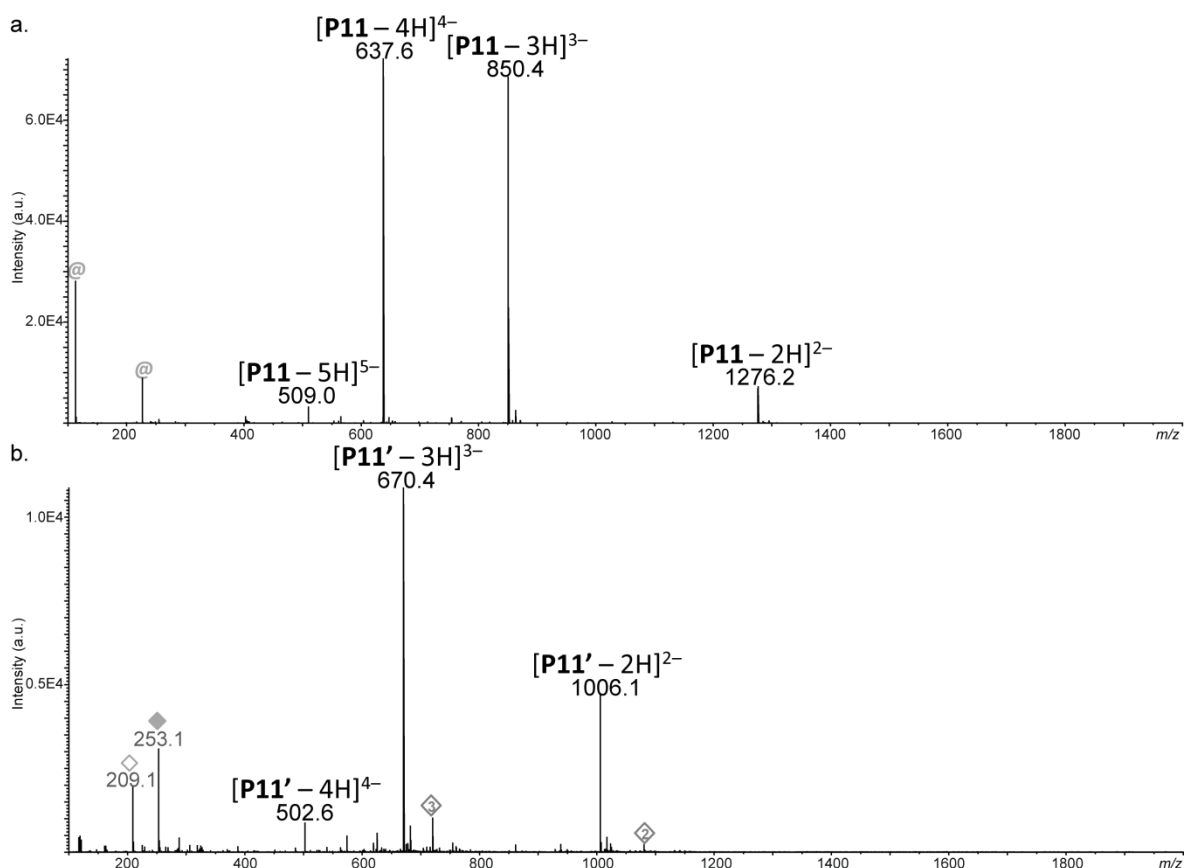
Supplementary Figure 40. MS/MS spectra recorded for copolymer **P7'** obtained after irradiation of **P7**, using a 28 eV collision energy (laboratory frame) to activate the triply deprotonated precursor at m/z 670.4. Peaks annotated in grey correspond to secondary fragments, including the deprotonated units, $[0 - \text{H}]^-$ at m/z 153.0 and $[1 - \text{H}]^-$ at m/z 288.0, both designated by #. Inset Table: Sequence coverage of **P7'** (*n.d.*: not detected; *n.e.*: not expected). Before photo-exposure, copolymer **P7** exhibits the same MS/MS spectrum as **P10** in Supplementary Figure 35.



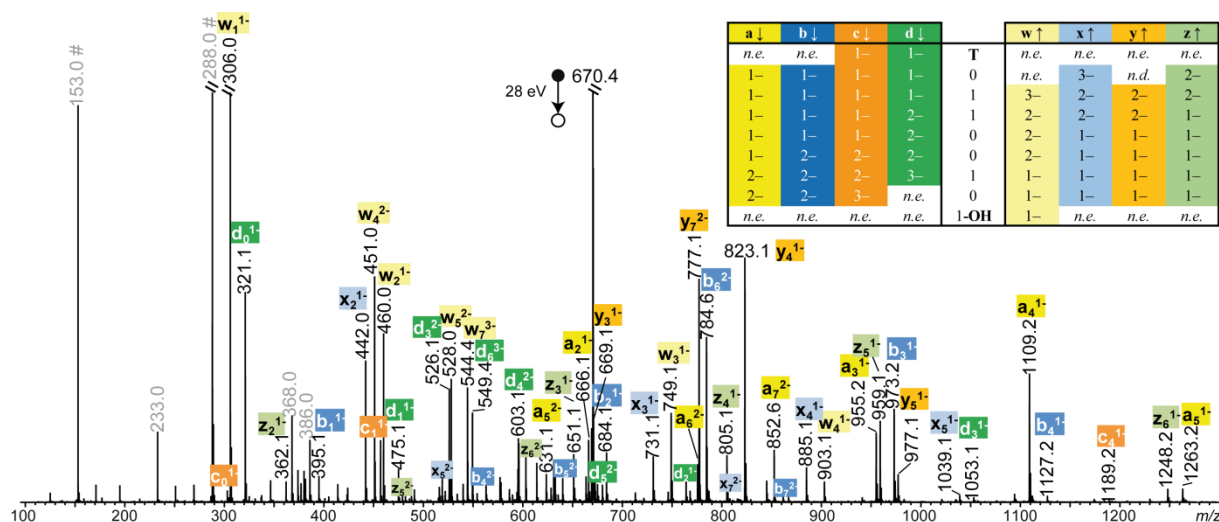
Supplementary Figure 41. ESI HRMS spectra recorded for (a) copolymer **P8** before irradiation and (b) the resulting polymer **P8'** after photo-exposure. Grey symbols designate clusters of trifluoroacetic acid (@) or photo-deprotection by-products (diamonds).



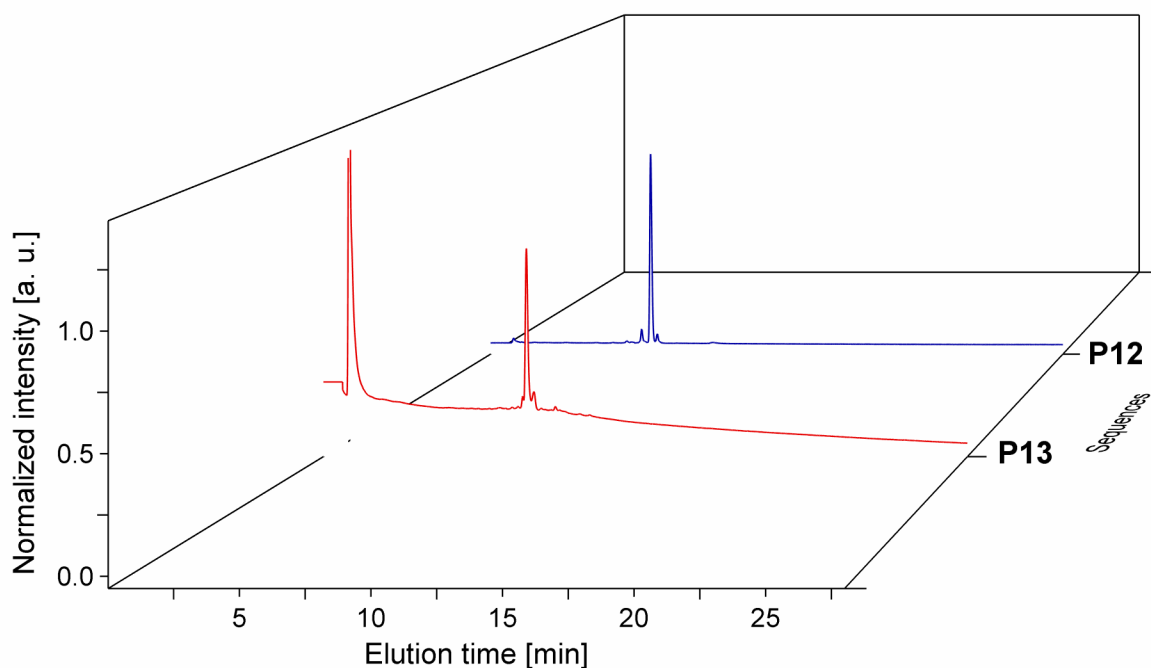
Supplementary Figure 42. MS/MS spectra recorded for copolymer **P8'** obtained after irradiation of **P8**, using a 25 eV collision energy (laboratory frame) to activate the triply deprotonated precursor at m/z 625.4. Peaks annotated in grey correspond to secondary fragments, including the deprotonated units, $[0 - \text{H}]^{-}$ at m/z 153.0 and $[1 - \text{H}]^{-}$ at m/z 288.0, both designated by #. Inset Table: Sequence coverage of **P8'** (n.d.: not detected; n.e.: not expected). Before photo-exposure, copolymer **P8** exhibits the same MS/MS spectrum as **P10** in Supplementary Figure 35.



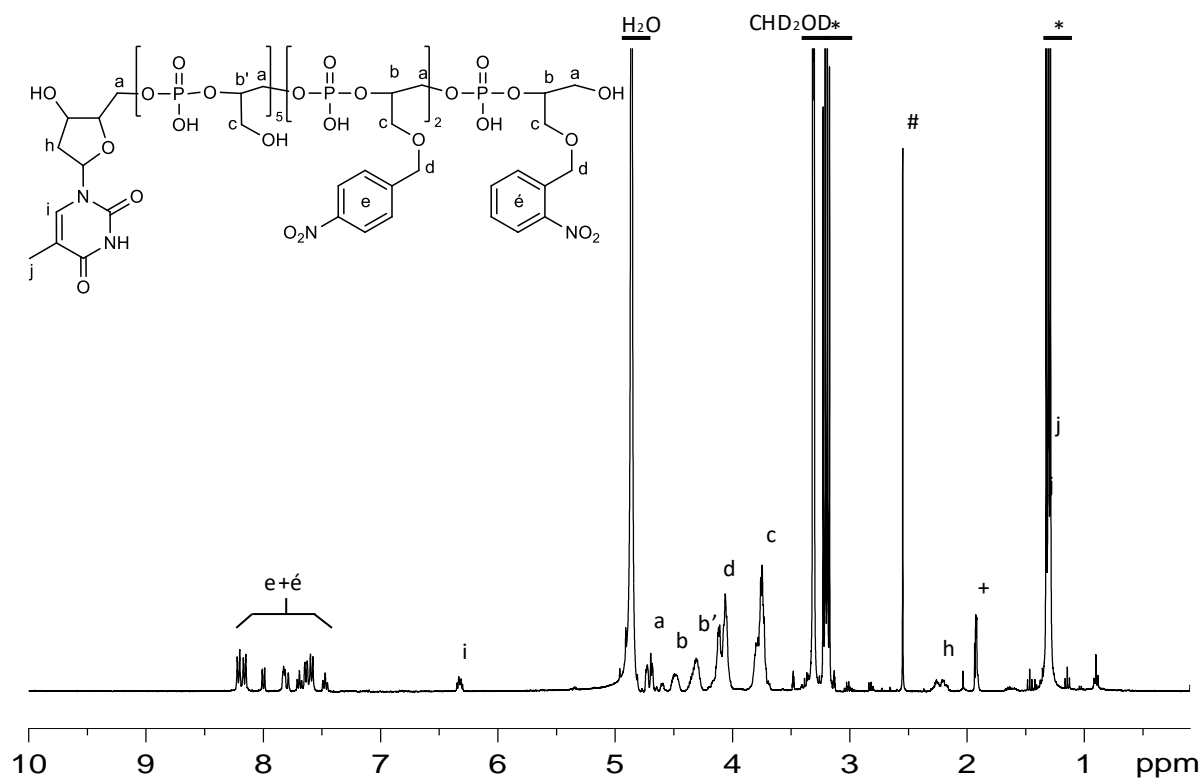
Supplementary Figure 45. ESI HRMS spectra recorded for (a) copolymer **P11** before irradiation and (b) the resulting polymer **P11'** after photo-exposure. Grey symbols designate clusters of trifluoroacetic acid (@) or photo-deprotection by-products (diamonds).



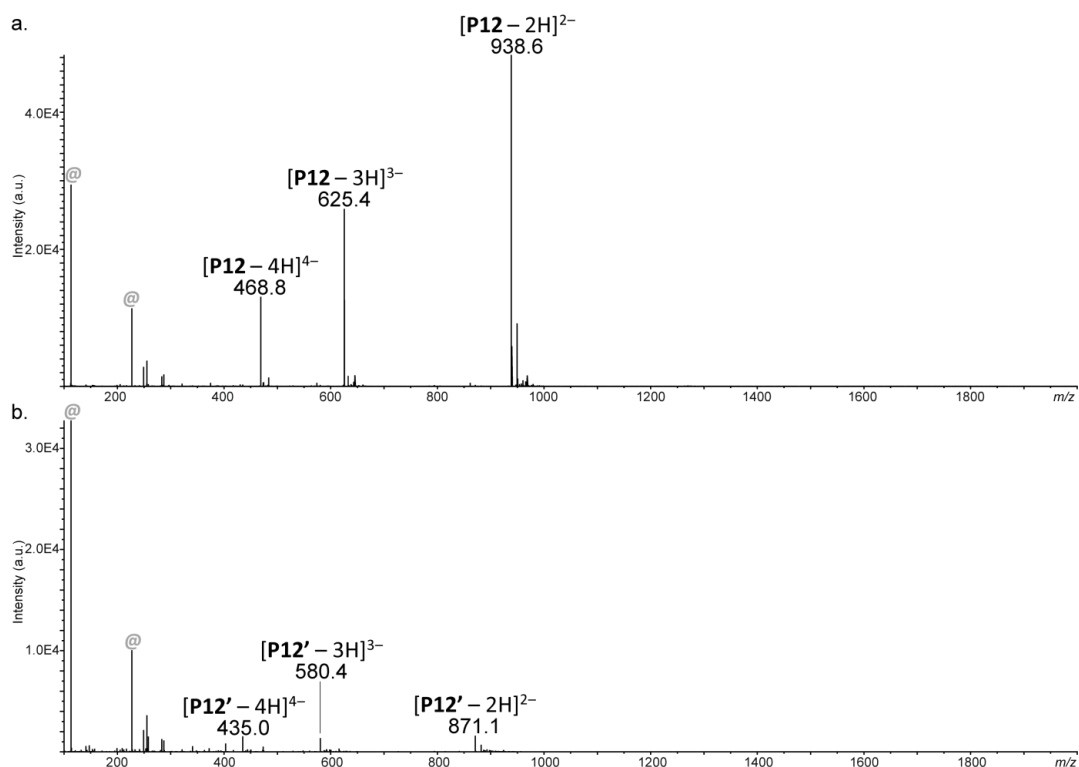
Supplementary Figure 46. MS/MS spectra recorded for copolymer **P11'** obtained after irradiation of **P11**, using a 28 eV collision energy (laboratory frame) to activate the triply deprotonated precursor at m/z 670.4. Peaks annotated in grey correspond to secondary fragments, including the deprotonated units, $[0 - \text{H}]^-$ at m/z 153.0 and $[1 - \text{H}]^-$ at m/z 288.0, both designated by #. Inset Table: Sequence coverage of **P11'** (*n.d.*: not detected; *n.e.*: not expected). Before photo-exposure, copolymer **P11** exhibits the same MS/MS spectrum as **P10** in Supplementary Figure 35.



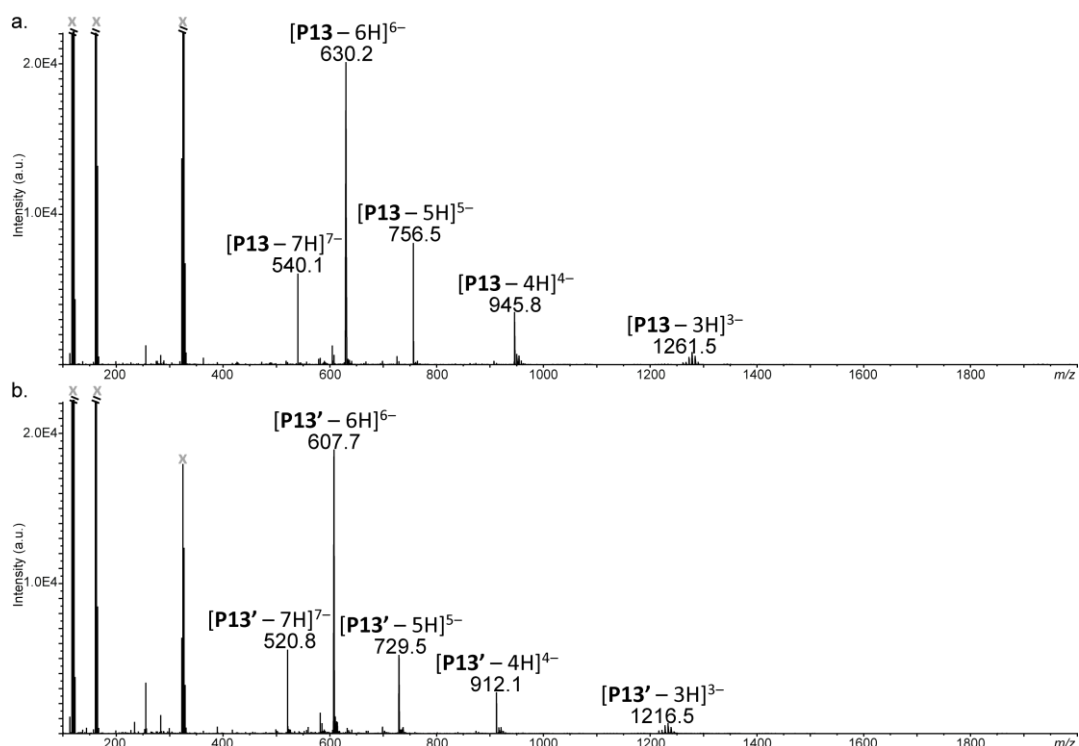
Supplementary Figure 47. HPLC traces measured for copolymers **P12** and **P13**. The chromatogram is recorded at $\lambda=260$ nm. Experimental conditions: phase A: 10 % ACN 20 % 2M NH_3 in water, phase B: 2.5 M NaCl in water; gradient: 0-3 min 5 % B, 3-23 min 5 % B-30 % B, 23-28 min 30 % B, 28-35 min 30% \rightarrow 5 % B; flow rate: $1 \text{ mL} \cdot \text{min}^{-1}$.



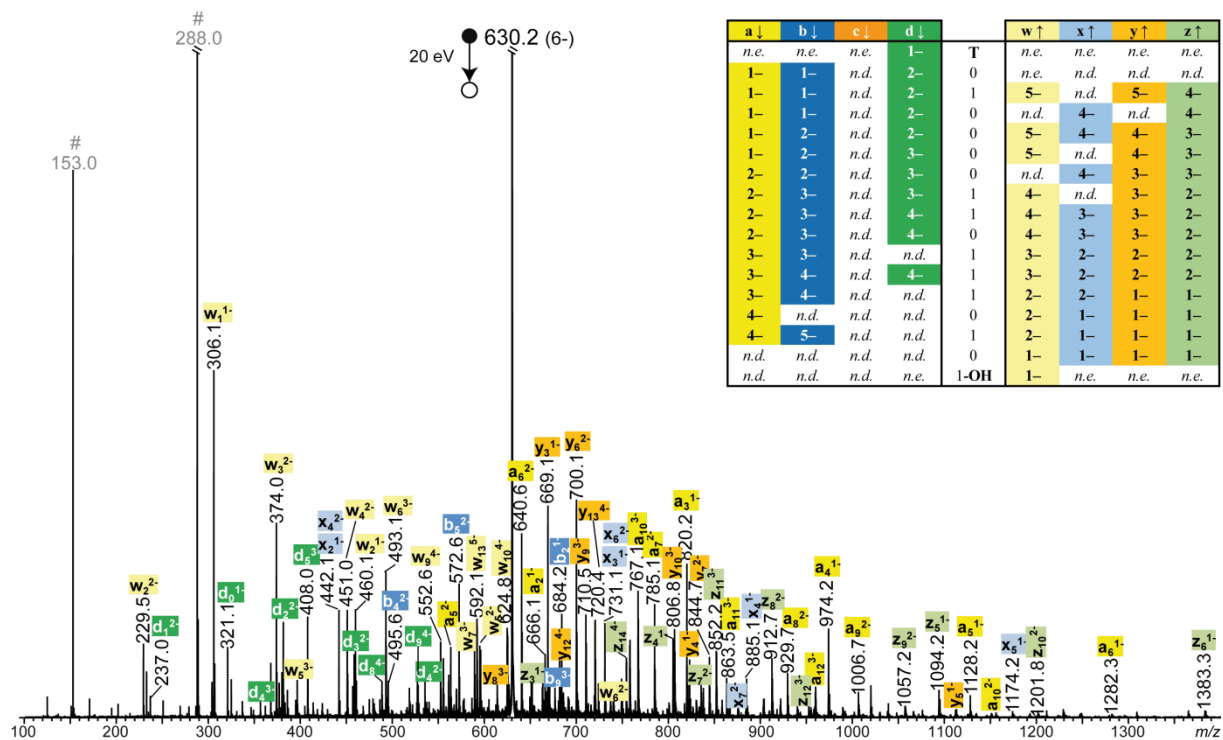
Supplementary Figure 48. ^1H NMR spectrum recorded at RT in CD_3OD for copolymer **P12**. The star symbols indicate signals of triethylammonium counterions. (#) Methylamine, (+) acetonitrile.



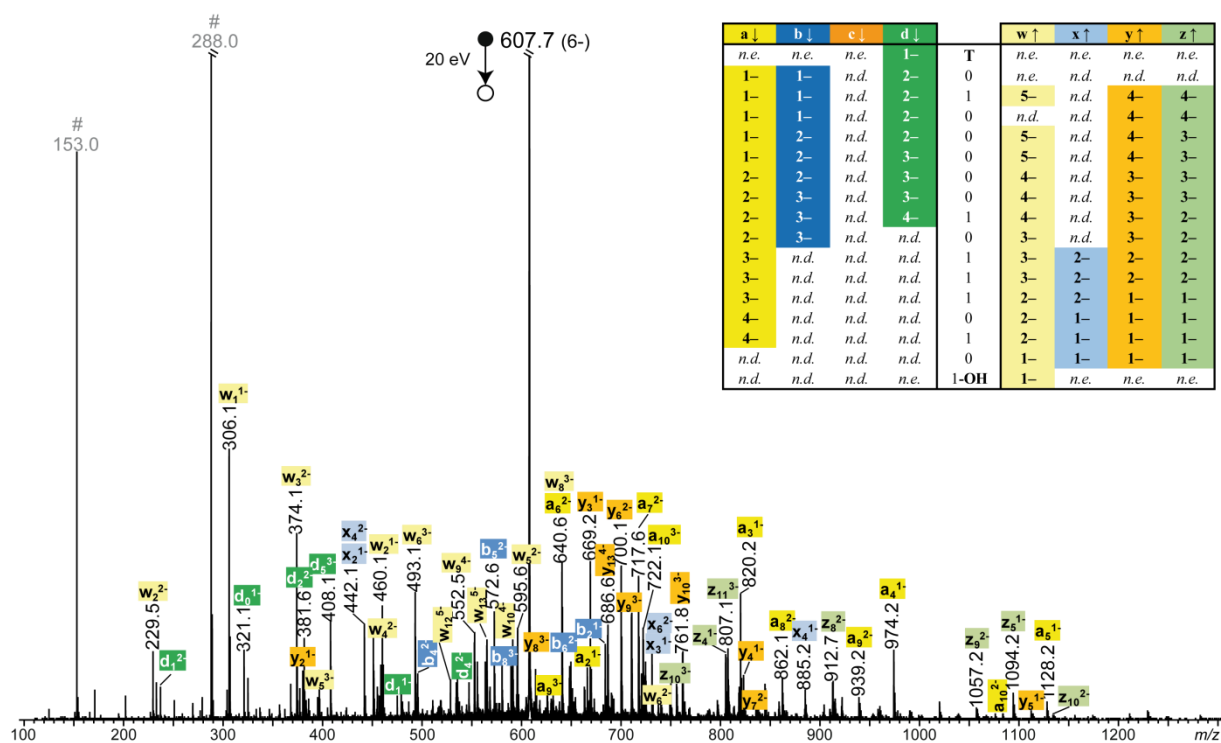
Supplementary Figure 49. ESI HRMS spectra recorded for (a) copolymer **P12** before irradiation and (b) the resulting polymer **P12'** after photo-exposure. Grey symbols indicate trifluoroacetic acid clusters (@).



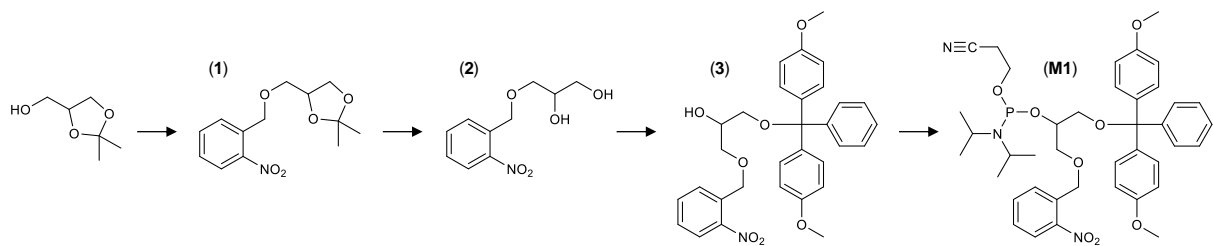
Supplementary Figure 50. ESI HRMS spectra recorded for (a) copolymer **P13** before irradiation and (b) the resulting polymer **P13'** after photo-exposure. Numerous H/Na exchanges in the lowest charge state species account for the more complex pattern observed for the 3⁻ ions. Grey symbols designate clusters of trifluoroacetic acid (x).



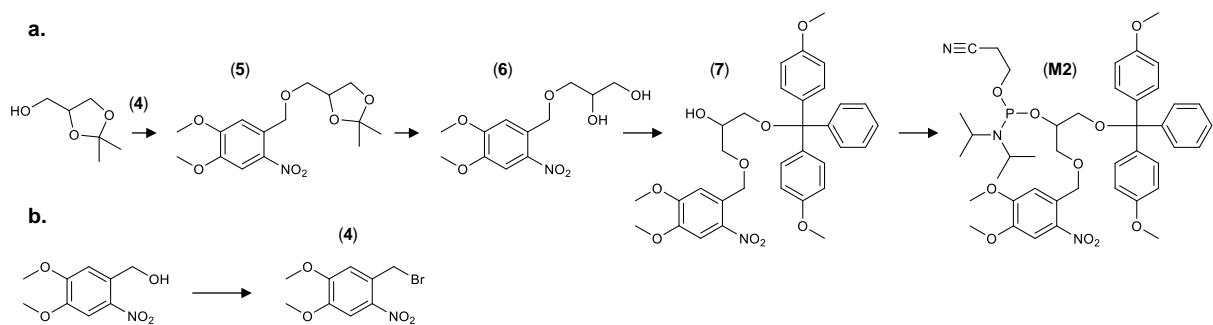
Supplementary Figure 51. MS/MS spectra recorded for copolymer **P13** before irradiation, using a 20 eV collision energy (laboratory frame) to activate the $[\mathbf{P13} - 6\text{H}]^{6-}$ precursor at m/z 630.2. In grey: secondary fragments, including the deprotonated units, $[0 - \text{H}]^-$ at m/z 153.0 and $[1 - \text{H}]^-$ at m/z 288.0, both designated by #. Inset Table: Sequence coverage of **P13** (*n.d.*: not detected; *n.e.*: not expected), with detailed assignments reported in Supplementary Table 7.



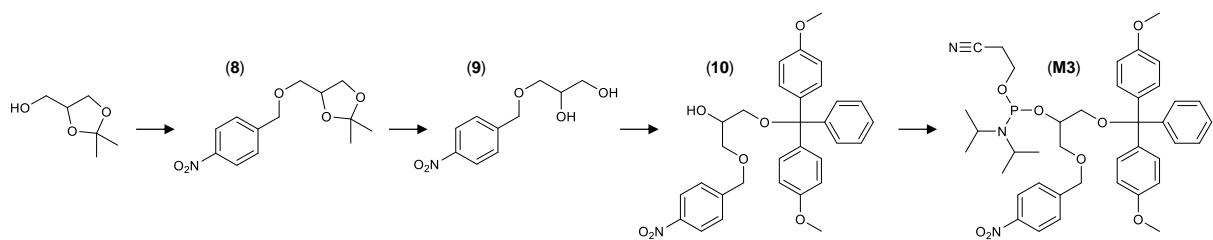
Supplementary Figure 52. MS/MS spectra recorded for copolymer **P13'** obtained after irradiation of **P13**, using a 20 eV collision energy (laboratory frame) to activate $[\mathbf{P13}' - 6\text{H}]^{6-}$ at m/z 607.7. In grey: secondary fragments, including the deprotonated units, $[0 - \text{H}]^-$ at m/z 153.0 and $[1 - \text{H}]^-$ at m/z 288.0, both designated by #. Inset Table: Sequence coverage of **P13'** (*n.d.*: not detected; *n.e.*: not expected), with detailed assignments reported in Supplementary Table 8.



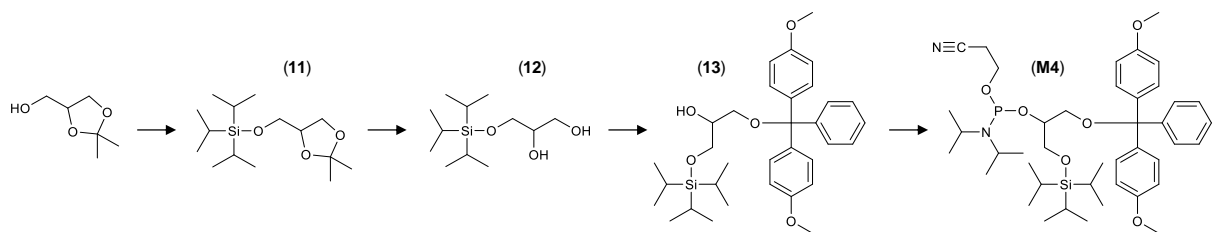
Supplementary Figure 53. Synthetic route used in this work for the preparation of **M1**.



Supplementary Figure 54. Synthetic route used in this work for the preparation of **M2**: (a) main synthesis route; (b) synthesis of 4,5-dimethoxy-2-nitrobenzyl bromide.



Supplementary Figure 55. Synthetic route used in this work for the preparation of **M3**.



Supplementary Figure 56. Synthetic route used in this work for the preparation of **M4**.

Supplementary Tables.

Supplementary Table 1. ESI-HRMS characterization of photo-erasable polymers.

Before irradiation				After irradiation			
	Sequence ^a	m/z_{th} ^b	m/z_{exp}		Sequence ^a	m/z_{th} ^b	m/z_{exp} ^c
H1	T 00000000	850.4499	850.4451	H1'	T ●●●●●●●●	490.3644	490.3584
H2	T 11111111	1010.5062	1010.5081	H2'	T ●●●●●●●●	490.3644	<i>n.d.</i> ^d
P1	T 01000101	910.4710	910.4710	P1'	T ●●●●●●●●	490.3644	490.3555
P2	T 01110010	930.4780	930.4785	P2'	T ●●●●●●●●	490.3644	490.3559
P3	T 01100001	910.4710	910.4711	P3'	T ●●●●●●●●	490.3644	490.3589
P4	T 01110011	950.4851	950.4839	P4'	T ●●●●●●●●	490.3644	490.3585
P5	T 01100101	930.4780	930.4795	P5'	T ●●●●●●●●	490.3644	490.3573

^a Before irradiation, bits 0 and 1 correspond to monomers **M1** and **M2**, respectively. After irradiation, the symbol ● represents the monomer unit of a non-decodable homopolymer. ^b The displayed m/z values correspond to $[M-3H]^3$. ^c After irradiation, targeted species were of too low abundance to allow high accuracy mass measurements, accounting for relative error of 10-20 ppm. ^d Due to its very low abundance, the triply deprotonated **H2'** polymer could not be accurately mass measured (*n.d.*: not determined).

Supplementary Table 2. ESI-HRMS characterization of polymers coded with an invisible ink.

Before irradiation				After irradiation			
	Sequence ^a	m/z_{th} ^b	m/z_{exp}		Sequence ^a	m/z_{th} ^b	m/z_{exp}
H3	T 11111111	850.4499	850.4520	H3'	T 11111111	850.4499	850.4484
P6	T 11111111	850.4499	850.4504	P6'	T 01000101	625.3965	625.3934
P7	T 11111111	850.4499	850.4527	P7'	T 01111000	670.4072	670.4061
P8	T 11111111	850.4499	850.4489	P8'	T 01110000	625.3965	625.3924
P9	T 11111111	850.4499	850.4538	P9'	T 01101111	760.4285	760.4254
P10	T 11111111	850.4499	850.4537	P10'	T 01110011	715.4178	715.4148
P11	T 11111111	850.4499	850.4522	P11'	T 01100101	670.4072	670.4073

^a Before irradiation, 1 and 1 correspond to isobaric monomers **M1** and **M3**, respectively. After irradiation, bit 0 corresponds to a photo-deprotected **M1** unit. ^b The displayed m/z values correspond to $[M-3H]^3$.

Supplementary Table 3. ESI-HRMS characterization of photo-mutable polymers.

Before irradiation				After irradiation			
	Sequence ^a	m/z_{th}	m/z_{exp}		Sequence ^a	m/z_{th}	m/z_{exp}
P12	T 01000011	938.5983 ^b	938.5995	P12'	T 01000010	871.0823 ^b	871.0818
P13	T 0100001101110101	756.4726 ^c	756.4720	P13'	T 0100000101110101	729.4662 ^c	729.4660

^a Before irradiation, 1 and 1 correspond to isobaric monomers **M1** and **M3**, respectively. Bit 0 corresponds to an OH-functional unit. ^b The displayed m/z values correspond to $[M-2H]^2$. ^c The displayed m/z values correspond to $[M-5H]^5$, measured at isotopic maximum.

Supplementary Table 4. Full coverage of the T01000101 sequence of **P1** using MS/MS data shown in Figure 2c.

a ↓	b ↓	c ↓	d ↓		w ↑	x ↑	y ↑	z ↑
<i>n.e.</i>	<i>n.e.</i>	1-	1-	T	<i>n.e.</i>	<i>n.e.</i>	<i>n.e.</i>	<i>n.e.</i>
1-	1-	1-	2-	0	<i>n.e.</i>	<i>n.d.</i>	2-	<i>n.d.</i>
1-	1-	<i>n.d.</i>	2-	1	2-/3-	3-	2-	2-
1-	2-	<i>n.d.</i>	<i>n.d.</i>	0	2-/3-	<i>n.d.</i>	2-	2-
1-	2-	<i>n.d.</i>	3-	0	2-/3-	2-	1-/2-	1-
1-/2-	2-	<i>n.d.</i>	<i>n.d.</i>	0	2-	<i>n.d.</i>	1-	1-
2-	2-/3-	<i>n.d.</i>	3-/4-	1	1-/2-	1-	1-	1-
2-/3-	<i>n.d.</i>	<i>n.d.</i>	<i>n.e.</i>	0	1-/2-	1-	1-	<i>n.d.</i>
<i>n.e.</i>	<i>n.e.</i>	<i>n.e.</i>	<i>n.e.</i>	1-OH	1-	<i>n.e.</i>	<i>n.e.</i>	<i>n.e.</i>

Values indicate the fragment charge state. *n.d.*: not detected. *n.e.*: not expected.

Supplementary Table 5. Full coverage of the T01110011 sequence of **P10'** using MS/MS data shown in Figure 3c.

a ↓	b ↓	c ↓	d ↓		w ↑	x ↑	y ↑	z ↑
<i>n.e.</i>	<i>n.e.</i>	1-	1-	T	<i>n.e.</i>	<i>n.e.</i>	<i>n.e.</i>	<i>n.e.</i>
1-	1-	1-	1-	0	<i>n.e.</i>	3-	<i>n.d.</i>	2-
1-	1-	1-	1-	1	3-	2-	2-	2-
1-	1-	1-	2-	1	2-	2-	2-	1-
1-	1-	2-	2-	1	2-	1-	1-	1-
1-	2-	2-	2-	0	2-	1-	1-	1-
2-	2-	2-	3-	0	1-	1-	1-	1-
2-	2-	3-	<i>n.e.</i>	1	1-	1-	1-	1-
<i>n.e.</i>	<i>n.e.</i>	<i>n.e.</i>	<i>n.e.</i>	1-OH	1-	<i>n.e.</i>	<i>n.e.</i>	<i>n.e.</i>

Values indicate the fragment charge state. *n.d.*: not detected. *n.e.*: not expected.

Supplementary Table 6. MS/MS data allowing full coverage of the T0100001X sequence of **P12** (X = 1) and **P12'** (X = 0).^a

	T	0	1	0	0	0	0	1	X	
i →	0	1	2	3	4	5	6	7	8	
a_i^{z-}	<i>n.e.</i>	<i>n.d.</i>	666.1 ¹⁻	820.2 ¹⁻	974.2 ¹⁻	1128.3 ¹⁻	1282.3 ¹⁻	785.2 ²⁻	<i>n.e.</i>	
b_i^{z-}	<i>n.e.</i>	395.1 ¹⁻	684.1 ¹⁻	838.2 ¹⁻	992.2 ¹⁻	1146.3 ¹⁻	1300.3 ¹⁻	794.2 ²⁻	<i>n.e.</i>	
c_i^{z-}	<i>n.e.</i>	457.1 ¹⁻	746.1 ¹⁻	900.2 ¹⁻	1054.2 ¹⁻	1208.2 ¹⁻	680.6 ²⁻	<i>n.d.</i>	<i>n.e.</i>	
d_i^{z-}	321.1 ¹⁻	475.1 ¹⁻	764.1 ¹⁻	918.2 ¹⁻	1072.2 ¹⁻	1226.2 ¹⁻	689.6 ²⁻	834.5 ²⁻	<i>n.e.</i>	
		8	7	6	5	4	3	2	1	← j
	<i>n.e.</i>	<i>n.e.</i>	749.6 ²⁻	1211.2 ¹⁻	1057.2 ¹⁻	903.2 ¹⁻	749.1 ¹⁻	595.1 ¹⁻	306.1 ¹⁻	
	<i>n.e.</i>	<i>n.e.</i>	682.1 ²⁻	1076.2 ¹⁻	922.1 ¹⁻	768.1 ¹⁻	614.1 ¹⁻	460.1 ¹⁻	171.1 ¹⁻	w_j^{z-}
	<i>n.e.</i>	817.6 ²⁻	1482.2 ¹⁻	1193.2 ¹⁻	1039.2 ¹⁻	885.2 ¹⁻	731.1 ¹⁻	577.1 ¹⁻	<i>n.e.</i>	
	<i>n.e.</i>	750.1 ²⁻	673.1 ²⁻	1058.1 ¹⁻	904.1 ¹⁻	750.1 ¹⁻	596.1 ¹⁻	442.1 ¹⁻	<i>n.e.</i>	x_j^{z-}
	<i>n.e.</i>	<i>n.d.</i>	1420.2 ¹⁻	1131.3 ¹⁻	977.2 ¹⁻	823.2 ¹⁻	669.1 ¹⁻	515.1 ¹⁻	<i>n.e.</i>	
	<i>n.e.</i>	719.1 ²⁻	1285.3 ¹⁻	996.2 ¹⁻	842.2 ¹⁻	688.1 ¹⁻	534.1 ¹⁻	380.1 ¹⁻	<i>n.e.</i>	y_j^{z-}
	<i>n.e.</i>	777.6 ²⁻	1402.3 ¹⁻	1113.3 ¹⁻	959.2 ¹⁻	805.2 ¹⁻	651.1 ¹⁻	497.1 ¹⁻	<i>n.e.</i>	
	<i>n.e.</i>	710.1 ²⁻	1267.3 ¹⁻	978.1 ¹⁻	824.2 ¹⁻	670.1 ¹⁻	516.1 ¹⁻	362.1 ¹⁻	<i>n.e.</i>	z_j^{z-}

^a For both polymers **P12** and **P12'**, α -terminated fragments (a_i , b_i , c_i , d_i) are identical since, in these series, species containing all units including the last X one (a_8 , b_8 , c_8 , d_8) are not expected to form (*n.e.*). In contrast, ω -terminated fragments (w_j , x_j , y_j , z_j) all contain the X unit as this is the first unit when counting from the right- to the left-hand side: accordingly, these series are different when X=1 for **P12** (m/z values in black) or X=0 for **P12'** (m/z values in red), with a mass shift corresponding to $m_1 - m_0 = 135$ Da.

n.d.: not detected.

Supplementary Table 7. MS/MS data allowing full coverage of the T0100001101110101 sequence of **P13**

(*n.e.*: not expected; *n.d.*: not detected).

i↓	$a_i^{z^-}$	$b_i^{z^-}$	$c_i^{z^-}$	$d_i^{z^-}$		$w_j^{z^-}$	$x_j^{z^-}$	$y_j^{z^-}$	$z_j^{z^-}$	
0	<i>n.e.</i>	<i>n.e.</i>	<i>n.e.</i>	321.1 ¹⁻	T	<i>n.e.</i>	<i>n.e.</i>	<i>n.e.</i>	<i>n.e.</i>	
1	377.1 ¹⁻	395.1 ¹⁻	<i>n.d.</i>	237.0 ²⁻	0	<i>n.d.</i>	<i>n.d.</i>	<i>n.d.</i>	<i>n.d.</i>	16
2	666.2 ¹⁻	684.2 ¹⁻	<i>n.d.</i>	381.5 ²⁻	1	680.7 ⁵⁻	<i>n.d.</i>	664.7 ⁵⁻	826.6 ⁴⁻	15
3	820.2 ¹⁻	838.2 ¹⁻	<i>n.d.</i>	458.6 ²⁻	0	<i>n.d.</i>	619.3 ⁴⁻	<i>n.d.</i>	754.4 ⁴⁻	14
4	974.2 ¹⁻	495.6 ²⁻	<i>n.d.</i>	535.6 ²⁻	0	592.1 ⁵⁻	735.9 ⁴⁻	720.4 ⁴⁻	954.8 ³⁻	13
5	1128.2 ¹⁻	572.6 ²⁻	<i>n.d.</i>	408.0 ³⁻	0	561.3 ⁵⁻	<i>n.d.</i>	681.9 ⁴⁻	903.5 ³⁻	12
6	640.6 ²⁻	649.6 ²⁻	<i>n.d.</i>	459.4 ³⁻	0	<i>n.d.</i>	658.8 ⁴⁻	858.2 ³⁻	852.2 ³⁻	11
7	785.1 ²⁻	529.1 ³⁻	<i>n.d.</i>	555.6 ³⁻	1	624.8 ⁴⁻	<i>n.d.</i>	806.8 ³⁻	1201.8 ²⁻	10
8	929.7 ²⁻	625.4 ³⁻	<i>n.d.</i>	488.8 ⁴⁻	1	552.6 ⁴⁻	731.1 ³⁻	710.5 ³⁻	1057.2 ²⁻	9
9	1006.7 ²⁻	676.8 ³⁻	<i>n.d.</i>	527.3 ⁴⁻	0	480.3 ⁴⁻	634.7 ³⁻	614.1 ³⁻	912.7 ²⁻	8
10	767.1 ³⁻	773.1 ³⁻	<i>n.d.</i>	<i>n.d.</i>	1	589.4 ³⁻	875.6 ²⁻	844.7 ²⁻	835.7 ²⁻	7
11	863.5 ³⁻	651.8 ⁴⁻	<i>n.d.</i>	537.2 ⁵⁻	1	493.1 ³⁻	731.1 ²⁻	700.1 ²⁻	691.1 ²⁻	6
12	959.8 ³⁻	724.1 ⁴⁻	<i>n.d.</i>	<i>n.d.</i>	1	595.6 ²⁻	586.6 ²⁻	1112.2 ¹⁻	1094.2 ¹⁻	5
13	758.1 ⁴⁻	<i>n.d.</i>	<i>n.d.</i>	<i>n.d.</i>	0	451.0 ²⁻	885.1 ¹⁻	823.2 ¹⁻	805.2 ¹⁻	4
14	830.4 ⁴⁻	667.6 ⁵⁻	<i>n.d.</i>	<i>n.d.</i>	1	374.0 ²⁻	731.1 ¹⁻	669.2 ¹⁻	651.1 ¹⁻	3
15	<i>n.d.</i>	<i>n.d.</i>	<i>n.d.</i>	<i>n.d.</i>	0	460.1 ¹⁻	442.1 ¹⁻	380.1 ¹⁻	362.1 ¹⁻	2
16	<i>n.d.</i>	<i>n.d.</i>	<i>n.d.</i>	<i>n.e.</i>	1-OH	306.1 ¹⁻	<i>n.e.</i>	<i>n.e.</i>	<i>n.e.</i>	1

j↑

Supplementary Table 8. MS/MS data allowing full coverage of the T0100000101110101 sequence of **P13'** (*n.e.*: not expected; *n.d.*: not detected).

i↓	$a_i^{z^-}$	$b_i^{z^-}$	$c_i^{z^-}$	$d_i^{z^-}$		$w_j^{z^-}$	$x_j^{z^-}$	$y_j^{z^-}$	$z_j^{z^-}$	
0	<i>n.e.</i>	<i>n.e.</i>	<i>n.e.</i>	321.1 ¹⁻	T	<i>n.e.</i>	<i>n.e.</i>	<i>n.e.</i>	<i>n.e.</i>	
1	377.1 ¹⁻	395.1 ¹⁻	<i>n.d.</i>	237.0 ²⁻	0	<i>n.d.</i>	<i>n.d.</i>	<i>n.d.</i>	<i>n.d.</i>	16
2	666.2 ¹⁻	684.2 ¹⁻	<i>n.d.</i>	381.5 ²⁻	1	653.7 ⁵⁻	<i>n.d.</i>	797.4 ⁴⁻	792.9 ⁴⁻	15
3	820.2 ¹⁻	838.2 ¹⁻	<i>n.d.</i>	458.6 ²⁻	0	<i>n.d.</i>	<i>n.d.</i>	725.1 ⁴⁻	720.6 ⁴⁻	14
4	974.2 ¹⁻	495.6 ²⁻	<i>n.d.</i>	535.6 ²⁻	0	565.1 ⁵⁻	<i>n.d.</i>	686.6 ⁴⁻	909.8 ³⁻	13
5	1128.2 ¹⁻	572.6 ²⁻	<i>n.d.</i>	408.0 ³⁻	0	534.2 ⁵⁻	<i>n.d.</i>	648.1 ⁴⁻	858.5 ³⁻	12
6	640.6 ²⁻	649.6 ²⁻	<i>n.d.</i>	459.4 ³⁻	0	629.6 ⁴⁻	<i>n.d.</i>	813.1 ³⁻	807.1 ³⁻	11
7	717.6 ²⁻	484.3 ³⁻	<i>n.d.</i>	510.7 ³⁻	0	691.1 ⁴⁻	<i>n.d.</i>	761.8 ³⁻	755.8 ³⁻	10
8	862.1 ²⁻	580.4 ³⁻	<i>n.d.</i>	455.1 ⁴⁻	1	552.6 ⁴⁻	<i>n.d.</i>	710.5 ³⁻	1057.2 ²⁻	9
9	939.2 ²⁻	631.7 ³⁻	<i>n.d.</i>	<i>n.d.</i>	0	480.3 ⁴⁻	<i>n.d.</i>	614.1 ³⁻	912.7 ²⁻	8
10	722.1 ³⁻	<i>n.d.</i>	<i>n.d.</i>	<i>n.d.</i>	1	589.4 ³⁻	875.6 ²⁻	844.7 ²⁻	835.5 ²⁻	7
11	818.5 ³⁻	<i>n.d.</i>	<i>n.d.</i>	<i>n.d.</i>	1	493.1 ³⁻	731.1 ²⁻	700.1 ²⁻	691.1 ²⁻	6
12	914.8 ³⁻	<i>n.d.</i>	<i>n.d.</i>	<i>n.d.</i>	1	595.6 ²⁻	586.6 ²⁻	1112.3 ¹⁻	1094.2 ¹⁻	5
13	724.4 ⁴⁻	<i>n.d.</i>	<i>n.d.</i>	<i>n.d.</i>	0	451.0 ²⁻	885.1 ¹⁻	823.2 ¹⁻	805.2 ¹⁻	4
14	796.6 ⁴⁻	<i>n.d.</i>	<i>n.d.</i>	<i>n.d.</i>	1	374.0 ²⁻	731.1 ¹⁻	669.2 ¹⁻	651.1 ¹⁻	3
15	<i>n.d.</i>	<i>n.d.</i>	<i>n.d.</i>	<i>n.d.</i>	0	460.1 ¹⁻	442.1 ¹⁻	380.1 ¹⁻	362.1 ¹⁻	2
16	<i>n.d.</i>	<i>n.d.</i>	<i>n.d.</i>	<i>n.e.</i>	1-OH	306.1 ¹⁻	<i>n.e.</i>	<i>n.e.</i>	<i>n.e.</i>	1

j↑

Supplementary References.

- 1 Klán, P., Šolomek, T., Bochet, C. G., Blanc, A., Givens, R., Rubina, M., Popik, V., Kostikov, A. & Wirz, J. Photoremovable Protecting Groups in Chemistry and Biology: Reaction Mechanisms and Efficacy. *Chem. Rev.* **113**, 119-191 (2013).
- 2 Barltrop, J. A., Plant, P. J. & Schofield, P. Photosensitive protective groups. *Chem. Commun.*, 822-823 (1966).
- 3 Patchornik, A., Amit, B. & Woodward, R. B. Photosensitive protecting groups. *J. Am. Chem. Soc.* **92**, 6333-6335 (1970).
- 4 Carré, P. Sur la décomposition de l'alcool ortho-nitrobenzylique sous l'influence de la soude aqueuse, et de la soude alcoolique. *C.R. Hebd. Seances Acad. Sci.* **140**, 663-665 (1905).